REPORT DOCUMENTATION PAGE

1a. REPORT SECURITY CLASSIFICATION UNCLASSIFIED	1b. RESTRICTIVE MARKINGS
2a. SECURITY CLASSIFICATION AUTHORITY	3. DISTRIBUTION/AVAILABILITY OF REPORT Approved for public release; distribution is unlimited.
2b. DECLASSIFICATION/DOWNGRADING SCHEDULE	
4. PERFORMING ORGANIZATION REPORT NUMBER(S)	5. MONITORING ORGANIZATION REPORT NUMBER(S)
6a. NAME OF PERFORMING ORGANIZATION Naval Postgraduate School 6b. OFFICE SYMBOL (*If applicable*) 35	7a. NAME OF MONITORING ORGANIZATION Naval Postgraduate School
6c. ADDRESS (*City, State, and ZIP Code*) Monterey, CA 93943-5000	7b. ADDRESS (*City, State, and ZIP Code*) Monterey, CA 93943-5000
8a. NAME OF FUNDING/SPONSORING ORGANIZATION 8b. OFFICE SYMBOL (*If applicable*)	9. PROCUREMENT INSTRUMENT IDENTIFICATION NUMBER
8c. ADDRESS (*City, State, and ZIP Code*)	10. SOURCE OF FUNDING NUMBERS Program Element No. / Project No. / Task No. / Work Unit Accession Number

11. TITLE (*Include Security Classification*)
AN INVESTIGATION OF THE GROUND-BASED HIGH-RESOLUTION INTERFEROMETER SOUNDER (GB-HIS) IN A COASTAL MARINE ENVIRONMENT

12. PERSONAL AUTHOR(S) Rugg, Steven A.

13a. TYPE OF REPORT	13b. TIME COVERED	14. DATE OF REPORT (*year, month, day*)	15. PAGE COUNT
Master's Thesis	From To	December 1992	100

16. SUPPLEMENTARY NOTATION
The views expressed in this thesis are those of the author and do not reflect the official policy or position of the Department of Defense or the U.S. Government.

17. COSATI CODES			18. SUBJECT TERMS (*continue on reverse if necessary and identify by block number*)
FIELD	GROUP	SUBGROUP	Remote Sensing, Coastal Meteorology, Interferometry, Atmospheric Profiling

19. ABSTRACT (*continue on reverse if necessary and identify by block number*)

Vertical temperature and moisture profiles from the Ground-Based High-Resolution Interferometer Sounder (GB-HIS) are studied for the coastal marine atmosphere. In May 1991 and 1992 the GB-HIS instrument was operated on the Research Vessel Point Sur during a cruise off the central California coast. The ability of the GB-HIS retrieval algorithm to produce accurate temperature and moisture profiles is evaluated using Root Mean Square (rms) difference, Bias, and Explained Variance statistics. In addition, objective analysis is performed on timesections of temperature and moisture. Temperature retrievals, on average, attained significant skill throughout the low troposphere. Moisture retrievals attained moderate skill in the lower and upper boundary layer, but no skill in the mid-boundary layer due to non-depiction of small moisture features. Results showed a maximum rms temperature difference of < 3 °C and rms dewpoint differences of < 12 °C in the low troposphere (up to 700 mb) over both cruises. Preliminary analysis of the updated retrieval algorithm is performed and further improvements are discussed.

T258504

20. DISTRIBUTION/AVAILABILITY OF ABSTRACT	21. ABSTRACT SECURITY CLASSIFICATION	
☒ UNCLASSIFIED/UNLIMITED ☐ SAME AS REPORT ☐ DTIC USERS	Unclassified	
22a. NAME OF RESPONSIBLE INDIVIDUAL Carlyle H. Wash	22b. TELEPHONE (*Include Area code*) (408)656-2295	22c. OFFICE SYMBOL MR/WX

DD FORM 1473, 84 MAR 83 APR edition may be used until exhausted
All other editions are obsolete

SECURITY CLASSIFICATION OF THIS PAGE
Unclassified

Approved for public release; distribution is unlimited.

An Investigation of the Ground-Based High-Resolution Interferometer Sounder (GB-HIS) in a Coastal Marine Environment

by

Steven A. Rugg
Captain, United States Air Force
B.S., University of Arizona, 1987

Submitted in partial fulfillment
of the requirements for the degree of

MASTER OF SCIENCE IN METEOROLOGY

from the

NAVAL POSTGRADUATE SCHOOL
December 1992

ABSTRACT

Vertical temperature and moisture profiles from the Ground-Based High-Resolution Interferometer Sounder (GB-HIS) are studied for the coastal marine atmosphere. In May of 1991 and 1992 the GB-HIS instrument was operated on the Research Vessel Point Sur during a cruise off the central California coast. The ability of the GB-HIS retrieval algorithm to produce accurate temperature and moisture profiles is evaluated using Root Mean Square (RMS) difference, Bias, and Explained Variance statistics. In addition, objective analysis is performed on timesections of temperature and moisture. Temperature retrievals, on average, attained significant skill throughout the low troposphere. Moisture retrievals attained moderate skill in the lower and upper boundary layer, but no skill in the mid-boundary layer due to non-depiction of small scale moisture features. Results showed a maximum RMS temperature difference of < 3 °C and RMS dewpoint difference of < 12 °C in the low troposphere (up to 700 mb) over both cruises. Preliminary analysis of the updated retrieval algorithm is performed and further improvements are discussed.

TABLE OF CONTENTS

ACKNOWLEDGMENTS

I would like to express my sincere thanks to Dr. Carlyle Wash, my thesis advisor, for his enthusiasm for this topic and his devotion to producing a quality investigative thesis. I was continually at his door and he was always willing to offer advice mixed with some much needed encouragement. My deep appreciation also goes to Dr. Ken Davidson who also provided much needed input to my thesis, and for sharing his expertise and eagerness for results. I am thankful for the patience of both men, especially for enduring this Air Force officer on a very active and unforgettable research cruise. Thanks also go to Mr. Jim Cowie and Mr. Kurt Nielsen who made using the IDEA Lab a pleasant and productive experience rather than a chore. Finally, I cannot forget the one who lived this thesis experience day in and day out with me, my wife Pamela. Her understanding of the missed dinners, her compassion for my frustrations, her never ending support when doubts appeared, and her prayers when I needed them the most only serve to reinforce in my mind how blessed I am to have her. This thesis is dedicated to her.

I. INTRODUCTION

Improvement in mesoscale weather prediction requires advances in instrumentation to observe meteorological phenomena on high temporal and spatial scales. High vertical resolution temperature and moisture soundings from geosynchronous or ground-based instruments are needed to make full use of the improved Doppler wind profiler observations planned for the 1990's (Smith et al. 1990). For mesoscale phenomena such as marine inversions or electromagnetic refractive (EMR) ducts aloft, it is important to have highly accurate and timely temperature and humidity distributions that together provide valuable information on vertical atmospheric structure.

This thesis will investigate the performance characteristics of the Ground-Based High-Resolution Interferometer Sounder (GB-HIS) in a coastal marine atmosphere. In this environment, a persistent marine boundary layer inversion often exists. Radar and microwaves used in the detection of enemy vessels or aircraft in the vicinity can be trapped by this inversion. Knowing when and where these inversions are can mean the difference between a surprise attack and a well-planned defense. The GB-HIS currently can provide accurate and consistent vertical temperature and

moisture profiles over land (Smith et al. 1990). The current goal is to improve the analysis and forecasting of these EMR ducts in the coastal zone plus other types of marine or coastal mesoscale events important to the Department of Defense (DOD).

The marine setting chosen for this investigation was on a research vessel (RV Point Sur) off the coast of central California. GB-HIS radiances were obtained on a near-continuous basis throughout each cruise. For comparison, in situ rawinsonde data was gathered at approximately 3 h to 6 h intervals on two separate research cruises, one occurring between the 8th through the 11th of May, 1992, and the other between the 7th through the 10th of May, 1991 respectively.

The objectives of this thesis are twofold. The first objective is to investigate the versatility and validity of the current GB-HIS retrieval algorithm for vertical temperature and moisture profiles as applied to a coastal marine environment using 1991 and 1992 Point Sur research cruise data. The second objective is to use the GB-HIS results to describe the evolution of temperature and dewpoint profiles and important tactical parameters (refractivity) for the two cruise cases.

II. THE GB-HIS INSTRUMENT

A. INSTRUMENT CHARACTERISTICS

A GB-HIS is a passive IR remote sensing device that can be either space-based or ground-based. As a ground-based instrument, it measures downwelling electromagnetic radiation across a near-continuous IR spectrum to produce relatively high resolution vertical temperature and moisture profiles within the planetary boundary layer (PBL) (Smith et al. 1992). The IR region over which a space-based GB-HIS measures its data (5 - 20 μm) is separated into three bands (Fig. 1): Band I (600-1080 cm^{-1}), Band II (1080-1850 cm^{-1}), and Band III (2000-

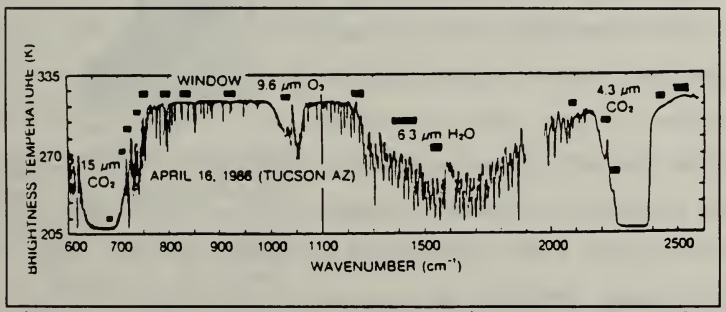

Figure 1: The IR spectrum over which the HIS samples its data as seen from a space-based instrument. Dark bars indicate GOES I/M VAS sensing bandwidths. This spectrum appears inverted for a ground-based instrument. (Smith et al. 1990)

2600 cm^{-1}) (Smith et al. 1990). The current ground-based GB-HIS separates the sampled IR spectrum into two bands, Band I from 600 cm^{-1} to 1500 cm^{-1} and Band II from 1500 cm^{-1} to 2600 cm^{-1}. As a result of the near-continuous monitoring over this large IR region, a virtual saturation of weighting functions occurs throughout the depth of the atmosphere, as seen in Fig. 2. This aids in obtaining high accuracy sounding retrievals. The best GB-HIS performance is found in the low troposphere between 0 to 2 km.

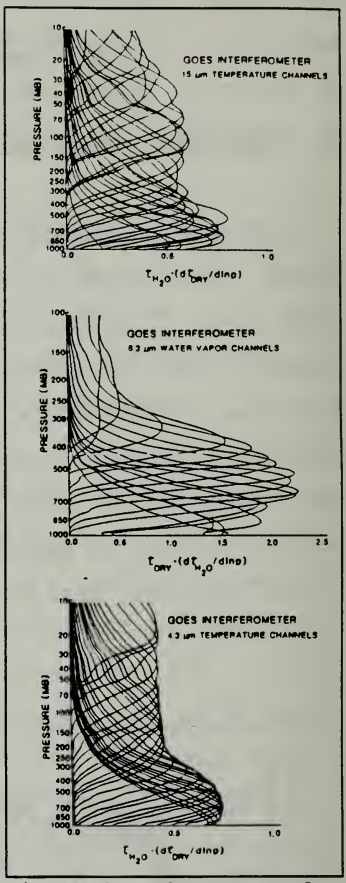

Figure 2: Three examples demonstrating the extent of the vertical saturation of weighting functions for the HIS. (Smith et al. 1990)

The sounding system developed at the University of Wisconsin (used in this investigation) includes a low cost Michelson Fourier transform interferometer, based on BOMEM (of Quebec, Canada) Michelson-100 technology, and a three point calibration system (Fig. 3). The Michelson interferometry technique is based on the varying speeds at which different electromagnetic waves

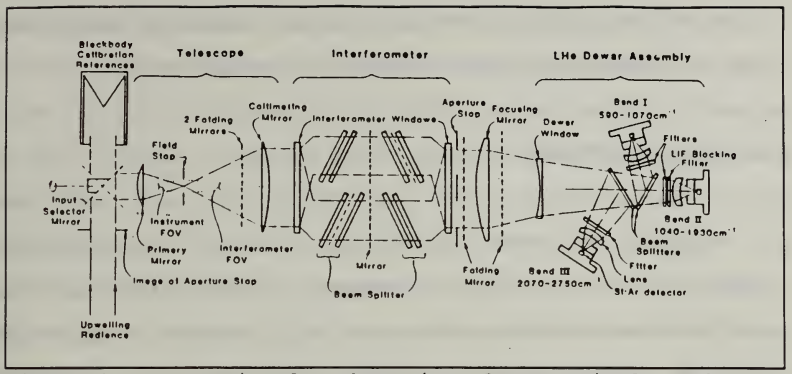

Figure 3: Functional schematic of a typical 3-channel Michelson interferometer. The primary, collimating and focusing mirrors are shown as lenses, and plane mirrors as dashed lines for simplification. (Revercomb et al. 1988)

travel in different media that splits the beam of radiation as it passes through a series of specially coated mirrors. These mirrors provide a "prism-like" effect on the IR radiation splitting the beam according to its component wavelength. Once split, the beams travel through another set of specially coated mirrors which alters, even more, the angle of incidence on the next mirror. Finally, the beams are reflected to a receiver which measures detect the range of wavelengths for each of the bands.

The calibration system consists of two high emissivity cavity blackbodies, one controlled at 333 K and the other which maintains an ambient temperature (280 - 295 K), and a third calibration source of a liquid nitrogen bath at 77 K (Smith et al. 1992). The scene switching mirror is controlled

by a processor to spend a preselected amount of time viewing the "sky" and any of the calibration positions.

B. DATA PROCESSING

Sounding retrieval algorithms are not overly computer intensive. In fact, ground-based interferogram data (i.e., the received radiance values) can be processed in "real-time" by local personal computers and used to retrieve atmospheric profiles of temperature and moisture. The sounding retrieval algorithm uses Fourier transformations and deconvolution of matrices of brightness temperatures to process data in accordance with the radiative transfer equation. A typical retrieval can be completed in three to five minutes from observation. There are nine user inputs to the current retrieval algorithm and three more are being added to the newest version of the algorithm (see Appendix). Choices made for each of these inputs affect the speed and quality of processing the radiance data. Optimum choices for these parameters remain under investigation. Users may vary the number of iterations desired, whether all of the IR spectrum is measured or only segments of it, and the maximum height of the sounding.

The retrieval algorithm which produces the atmospheric temperature and moisture soundings is composed of Fortran modules, some of which have code spliced into them from

FASCODE and LOWTRAN6. This algorithm can be run in two modes, either a single iterative mode or a multiple iterative mode. There is little information, to date, as to the effectiveness of the multiple iterative mode; however, preliminary results show more than nine iterations cause instabilities in the retrievals. Plus, for each additional iteration, the computational time to produce a sounding increases by a proportional amount (e.g., four iterations takes four times longer). The multiple iterative mode is still under investigation and consequently, the single iterative mode is predominately used at this time. Both modes allow for the use or nonuse of surface observations recorded from the observed radiance values and a toggle whether to apply the effects of aerosols in the retrieval. The effects of aerosols on the retrieval accuracy is still in the research stage; however, the aerosol module approximately doubles the time to obtain a sounding. Surface observations do increase the accuracy and add a small amount of time to the retrieval process.

C. SCALES AND ACCURACY

1. Vertical Scales

For the GB-HIS to be of value for the mesoscale applications, it must be accurate to at least the scale of existing instruments (i.e., rawinsondes). Using a space-based

system for example, previous GOES VAS data had a vertical resolution of 4 km at an altitude of 400 mb, twice that of the GB-HIS. The aspect ratio between horizontal and vertical wavelengths of atmospheric phenomena is approximately 100 to 1. Consequently, to resolve mesoscale features on the order of 200 km, 2 km vertical resolution must be attained (Smith et al. 1983). Also, to maintain an accuracy consistent with the Doppler radar wind profiler, it can be shown via the thermal wind relationship that the temperature and water vapor distribution must be observed with a vertical resolution of 1-2 km and an accuracy of 1 °C for temperature and 3 °C for dewpoint (Smith et al. 1990). Fig. 4 shows the vertical resolution capability of the GB-HIS in comparison to the GOES I/M filter instrument or VAS. The accuracy of vertical temperature profiles within the low troposphere, where the GB-HIS is most accurate, is extremely important to the reliability of stability parameters.

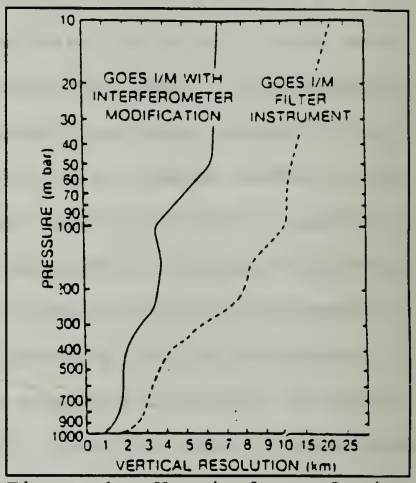

Figure 4: Vertical resolution of the HIS versus the GOES I/M filter wheel sounder (VAS). (Smith et al. 1990)

Closely tied to the concept of vertical resolution is the spectral resolution of the interferometer. The GB-HIS

must achieve near continuous spectral coverage throughout the 600-2600 cm^{-1} region to obtain high vertical resolution temperature and moisture profiles. For the interferometer to accomplish this, it must maintain a 0.1% ($\Delta\lambda/\lambda$) spectral resolution throughout the whole region to avoid "smearing" of the downwelling radiance contributions from relatively opaque absorption lines in comparison to relatively transparent regions in between those absorption lines (Smith et al. 1990). Spectral resolutions of 0.5, 1.0, and 1.5 cm^{-1} for Bands I, II, and III were obtained during GAPEX (Ground-Based Atmospheric Profiling Experiment) (Smith et al. 1990), proving the GB-HIS can attain the necessary spectral resolution.

2. Temporal Scales

A ground-based GB-HIS produces a completely calibrated and apodized spectra for processing every ten seconds. These spectra can then be averaged over any desired time interval to reduce radiometric noise and the data volume, and then subsequently processed to a produce vertical sounding (Smith et al. 1992). The time output spectra are averaged over is variable based on user needs. For example, a user can average over an hour and raise a "flag" when certain upper air criterion are met, or over 30 minutes to maintain a close watch on stability parameters for convective activity, or even every five minutes to maintain a constant vigil on developing

or decaying refractive ducts. Consequently, a GB-HIS more than meets the short-term time requirements for mesoscale weather prediction.

3. Accuracy

The accuracy of an instrument demonstrates the quality of its measurements and provides the confidence for its use. For example, GB-HIS temperature measurements determined during the Ground-Based Atmospheric Profiling Experiment (GAPEX) at Denver, Colorado have been shown to maintain 1 °C agreement with Cross-Chain LORAN Atmospheric Sounding System (CLASS) rawinsondes up to 650 mb (Smith et al. 1990). In comparison to the other two atmospheric profilers tested during GAPEX, the GB-HIS even demonstrated a minor improvement over a Microwave Profiler (MWP) and a Radio Acoustic Sounding System (RASS) as seen in Fig. 5. The GB-

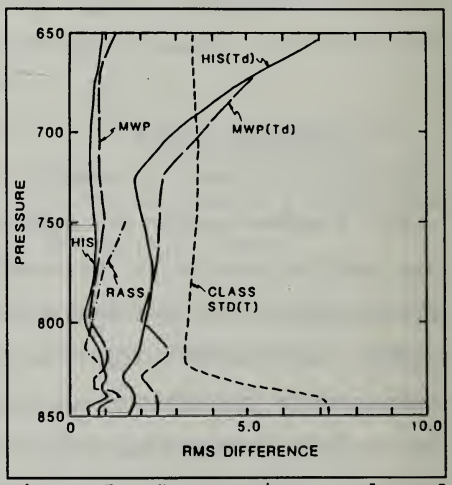

Figure 5: Comparative results of the HIS during the GAPEX with other surface based atmospheric profilers. RMS differences less than the CLASS standard deviation indicate skill. (Smith et al. 1990)

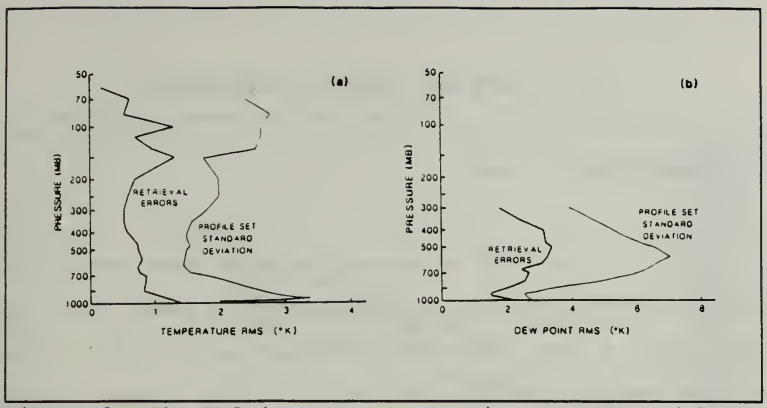

Figure 6: The RMS (root-mean-square) temperature (a) and dewpoint (b) error as a function of height compared to the CLASS rawinsondes standard deviation. (Smith et al. 1990)

HIS dewpoint measurements, while needing improvements above 700 mb, still out performed the MWP (Fig. 5). Also, in an airborne mode during COHMEX (Combined Huntsville Meteorological Experiment), Figs. 6 (a) and (b) show the required < 1 °C temperature resolution and < 3 °C dewpoint resolution for mesoscale effectiveness as stated earlier, along with marked skill throughout the atmosphere. Ground-based systems are expected to do as well.

III. DATA AND SYNOPTIC DISCUSSION

A. DESCRIPTION OF DATA

In May 1991 and 1992 a research cruises were completed by the Naval Postgraduate School using Research Vessel (RV) Point Sur. One of the areas of investigation of both cruises included validation of the GB-HIS in a coastal marine environment. The RV Point Sur cruise tracks covered central California coastal zone (Fig. 7) avoiding cloud cover as much as possible. The 1991 cruise period began at 07/1800Z and ended at 10/1400Z, providing useful data for investigation between 08/00Z to 10/13Z. Likewise, the 1992 cruise began at 08/20Z and ended at 11/13Z, providing useful data for investigation between 09/00Z to 10/24Z. The GB-HIS instrument used on the 1991 cruise was a single channel interferometer operating over the IR spectrum from 480 cm^{-1} to 1400 cm^{-1}. This instrument did not yet have the capability to record surface temperature onto the received radiance signal; however, the 1992 GB-HIS instrument did have this capability. The 1992 GB-HIS instrument was upgraded to a 2-channel interferometer with spectral limits for each channel as stated earlier in Chapter II. The GB-HIS instrument was located on the port side on the second deck so it would avoid any protruding structure of the

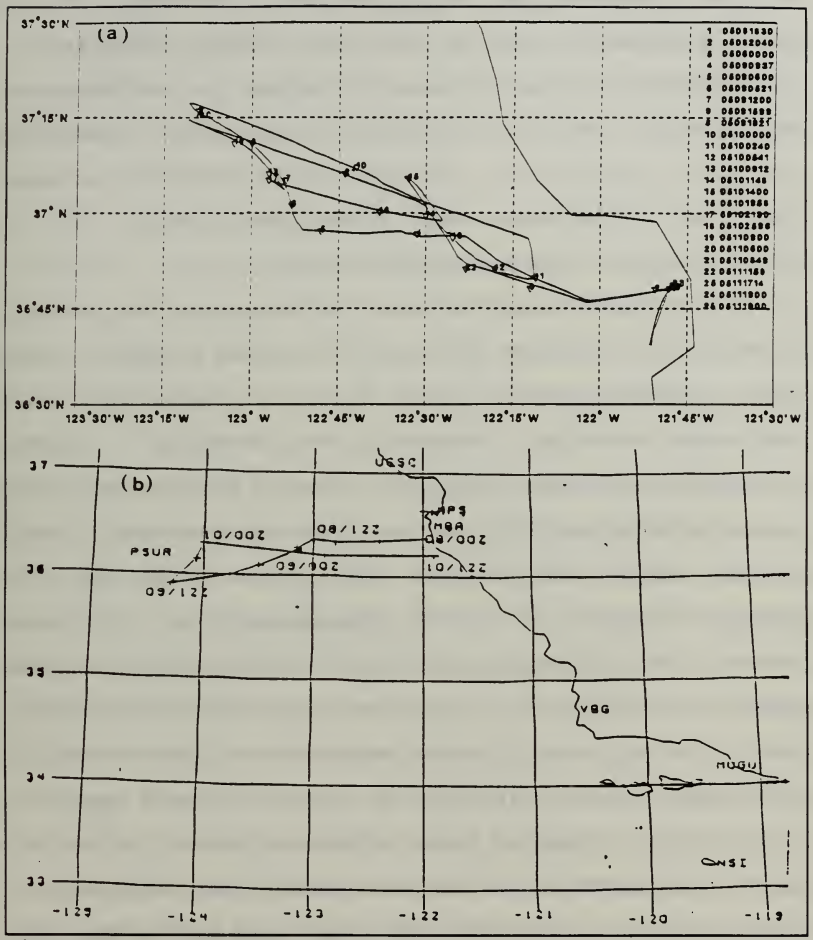

Figure 7: Plot of the ship paths for each of the research cruises. The 1992 cruise is in depicted in (a) and the 1991 cruise is in (b).

ship and yet be protected from sea spray. The GB-HIS instrument ran continuously, collecting radiances every 10 minutes throughout the 1992 cruise, but it was turned off for brief periods of time on the 1991 cruise. Vaisala Inc. rawinsondes were launched every 6 h during the 1991 cruise and approximately every 3 h during the 1992 cruise. The GB-HIS radiance values were computed by the GB-HIS retrieval algorithm to produce temperature and moisture profiles corresponding to the rawinsonde profiles.

The retrieval algorithm run for both years data used a smoothed initial guess profile. The guess profiles during this investigation for each day were always the 0000Z rawinsonde sounding. Smoothing was necessary to prevent instabilities in the retrieval. Certain sections of the IR spectrum were also blocked out from use because of their opacity due to water vapor. Since this investigation is mainly interested in the low troposphere (i.e., 700 mb and below), the retrievals were forced to merge with the first guess rawinsonde profile at 600 mb to lessen the computational time. The retrieval algorithm was allowed to perform only one iteration and the effects of marine aerosols were not accounted for. Both are areas for further investigation. The surface temperature observations in the observed radiances, available only in the 1992 data, were used in the retrievals for the 1992 cruise, but not for the 1991 cruise.

B. DESCRIPTION OF SYNOPTIC CONDITIONS

The following is a description of the synoptic conditions encountered on the 1991 and 1992 Point Sur cruises. All times referred to in this discussion and throughout the rest of this document are in Greenwich Mean Time (GMT or Z) which is seven hours earlier than local time.

Fig. 8 provides general representation of the type of synoptic weather conditions encountered during the 1991 cruise. At the beginning of the cruise, the front depicted on Fig. 8 was to the northwest of RV Pt Sur. A pre-frontal marine inversion existed at this time with light and variable winds. As the front approached, the associated upward vertical motions caused the marine inversion to rise. The front passed overhead at approximately 08/1400Z eliminating the marine inversion. By 08/2100Z the frontal zone had completed its passage of the area leaving in its wake post-frontal cooling and strong mid-tropospheric subsidence which eventually extends to the surface. By 10/0000Z the marine inversion had reestablished itself once again. A more thorough discussion of the synoptic situation during the 1991 Point Sur cruise has been provided by Martinez (1991).

The 1992 cruise synoptic situation at 08/20Z had a strong 1034 mb surface high north of 40 °N and just west of 135 °W. This high was moving eastward and was showing signs of ridging into the northern Oregon/southern Washington area. Another

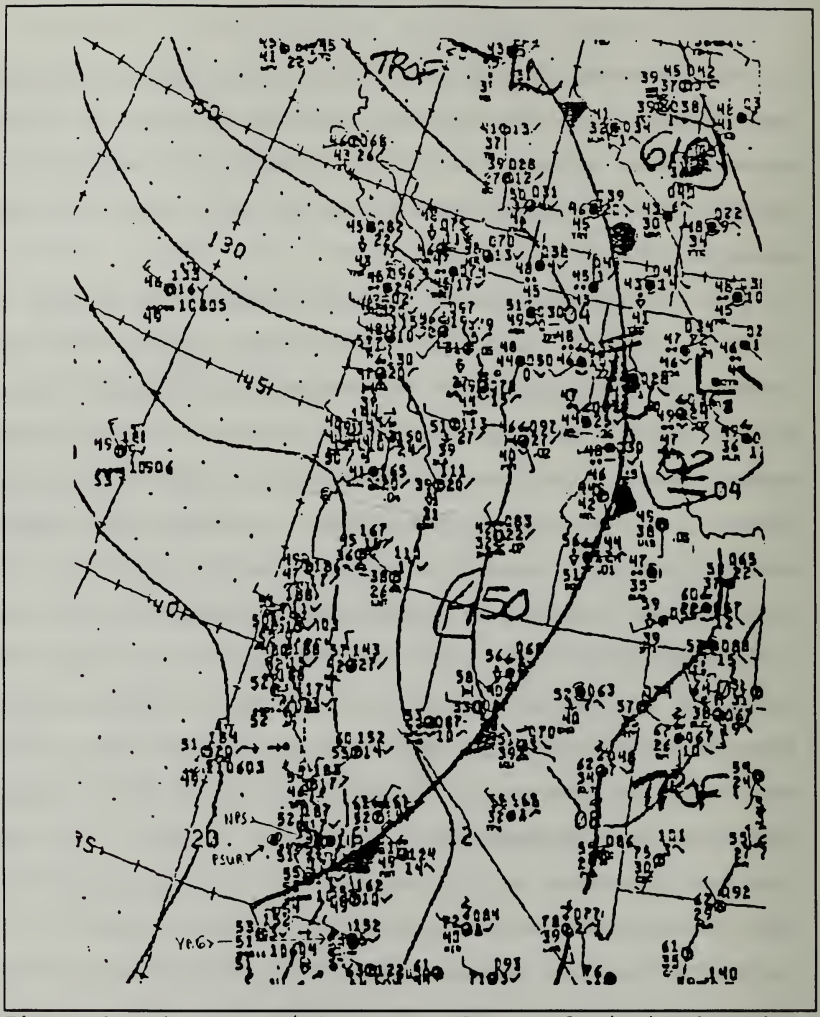

Figure 8: The 910508/1500 GMT surface analysis is shown here with the cold front just south of Monterey CA as the most significant synoptic feature. The position of RV Pt. Sur is also plotted.

high was located over the four corners region, but was much weaker at 1014 mb and had been slowly weakening throughout the day. Sandwiched in between these two surface highs was a long cold frontal system with its southern end on the California coast north of San Francisco, stretching across Reno, Nevada, central Idaho, Montana to a low center just north of the Montana/Canada border. Winds were light and variable, and the sky overcast stratus. By 09/00Z (Fig. 9), the low center associated with the front moved southeastward and the southern end of the front moved further north of San Francisco.

The high centered over the four corners remained in place at 1014 mb. The high off the northwest coast continued to move east and strengthened the pressure gradient in Oregon, Idaho, and Washington, behind the cold front and along the coast of California. Because of the increasing pressure gradient along the coast, strong north-northwest winds developed at 25 to 30 knots. After several hours of intense offshore flow, skies cleared around 09/02Z. By 09/12Z, as the western high pressure system continued to progress into northern Nevada and Idaho the cold front moved eastward into central Wyoming, central Utah, and southern Nevada with its southern end parallel to the California coast just east of San Francisco. The offshore pressure gradient maintained its strength during the remainder of the cruise with winds steadily above 25 knots gusting to 40 knots at times. Skies also remained scattered to clear during this time period. By

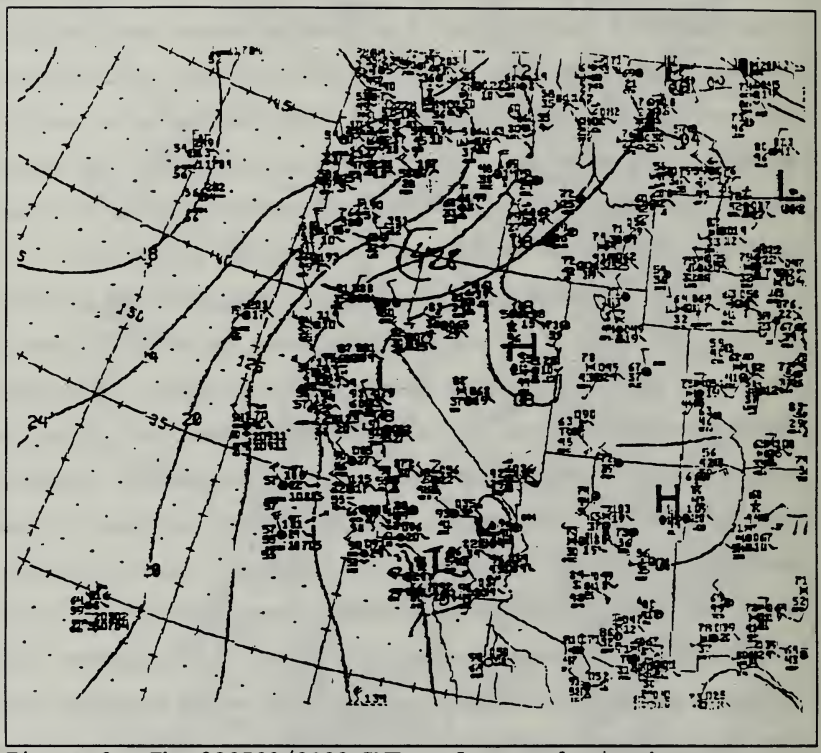

Figure 9: The 920509/0000 GMT surface analysis shows a strong pressure gradient off the California coast creating a strong offshore flow. This regime predominated throughout most of the cruise.

10/00Z, the only change in the synoptic situation is the cold front had moved even farther southeastward into northern Colorado, southern Utah, and northern Arizona. Strong northerly winds (25 to 35 knots) and scattered skies continued. Up to 10/12Z, sky coverage remained clear while winds persisted from the north, but diminished slightly to 20 knots.

Around 10/12Z, a weak low pressure center developed over the San Francisco Bay and Monterey Bay area. Wind speed dropped dramatically, down to 5 to 10 knots, and changed direction, coming out of the south. As a result of this wind shift, a stratus overcast slowly moved in and overtook the ship by 10/17Z. The ship was maneuvered west to transit out from under the stratus overcast. By 10/20Z, the ship had returned to scattered skies and by 10/22Z light northerly winds reappeared. A broad high pressure system began to build over the coast of California throughout the remainder of the cruise from 11/00Z to 11/13Z. This brought light and variable winds with scattered to clear skies. However, it also reestablished the onshore return flow, which brought overcast stratus over the ship at 11/09Z. As the cruise ended, the influence of the weak low pressure trough over all of California caused southerly winds of 5 to 10 knots. The visibility throughout the cruise never fell below seven miles, and no precipitation was encountered.

IV. EVALUATION OF GB-HIS RETRIEVALS

A. 1992 CRUISE

The GB-HIS retrievals will be evaluated using mini-rawinsonde data taken every 3 h on the 1992 cruise and every 6 h on the 1991 cruise. Initially, a timesection format will illustrate similarities and differences between the two types of measurements. Then, a statistical analysis will be completed on the differences between the GB-HIS and the mini-rawinsonde data.

1. Rawinsonde Timesections (9 May 92)

The dominant feature of low-troposphere in the 1992 cruise is the presence of a strong marine inversion. Timesections of temperature from rawinsondes and GB-HIS retrievals from 9 May 92 (Fig. 10a) show the maximum temperature at the top of the inversion is approximately 296 K occurring near 03Z and 09Z. Later in the period (12Z to 20Z), the temperature at the top of the inversion decreases to 293 K. The top of the inversion is at about 930 mb at the beginning of the period. By 03Z, the top of the marine inversion rises slightly to 925 mb and then gradually descends to approximately 950 mb just after 12Z. A very strong

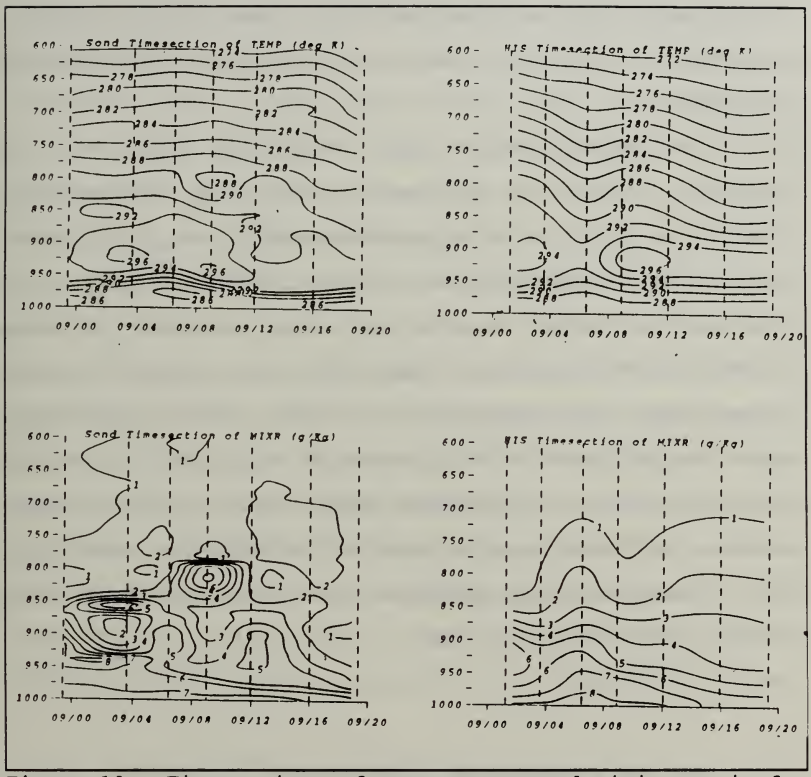

Figure 10: Timesections of temperature and mixing ratio for the rawinsonde, (a) and (c), and the GB-HIS, (b) and (d), over the period of 920509/0000 GMT to 920509/2400 GMT. Mixing ratio is in g/Kg and temperature is in °K.

vertical temperature gradient from the base to the top of the marine inversion was evident throughout the period. Relative cold pockets are just above the top of the inversion at a height of 850 mb between 00Z to 03Z, at the 800 mb level (09Z) and at 850 mb between 12Z and 16Z. Except for this small scale detail, there is a rather uniform lapse rate from 800 mb to 600 mb.

The surface moist layer, which is capped by the inversion, is one of the main features of the moisture timesection (Fig. 10c). At the beginning of the day (03Z), a distinct narrow moist layer is near the base of the marine inversion at 950 mb. A 50 mb dry layer is found just above the base of the inversion. Just above this dry layer, another narrow moist layer is present at 850 mb. The surface moist layer narrows from 06Z to the end of the period, but still detectable, with a noticeable, gradual decrease in moisture. A marked, elevated layer of moist air is at 800 mb centered on 09Z. Other than these occasional thin moist layers, moisture content above 850 mb is small.

2. GB-HIS Timesections (9 May 92)

The GB-HIS, initialized at 0000Z, also detects an inversion on the temperature timesection (Fig. 10b), locating the top at 925 mb from 00Z to 09Z with an initial maximum 295

K. From 09Z to 12Z the inversion height remains the same, but the maximum temperature increases to 297 K. The maximum temperature at the top of the inversion drops to 295 K, while the height again remains unchanged. No relative cold or warm regions other than near the inversion are detected. A moderate and uniform lapse rate is observed across the inversion. Also, a smooth and uniform lapse rate occurs above 850 mb. A comparison of the rawinsonde and GB-HIS measurements show that the GB-HIS provides a successful analysis of the boundary temperatures on 9 May.

The GB-HIS also measures the strong moist surface layer on 9 May (Fig. 10d), but it is not as sharply defined as by the rawinsonde. At the beginning of the day, there is moistening at the base of the inversion with only gradual drying through it to the top of the inversion and above. Gradual drying of the marine layer continues through the rest of the day. Throughout the whole day, the humidity decreases from the surface to 600 mb is smooth with the absence of any small scale (< 50 mb) moist layers that are present in the rawinsonde data. Little moisture is observed above 800 mb.

3. Rawinsonde Timesections (10 May 92)

On the second day of the 1992 cruise, the marine temperature inversion remains the striking feature as shown in the rawinsonde timesection (Fig. 11a). The maximum

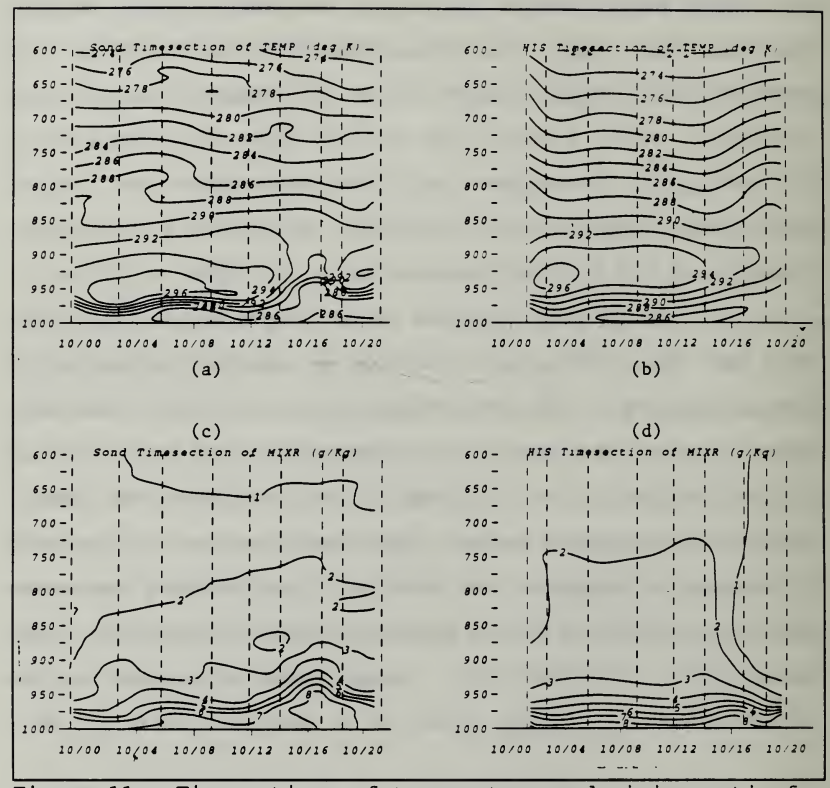

Figure 11: Timesections of temperature and mixing ratio for the rawinsonde, (a) and (c), and the GB-HIS, (b) and (d), over the period of 920510/0000 GMT to 920510/2400 GMT. Mixing ratio is in g/Kg and temperature is in °K.

temperature at the top of this inversion from 00Z to 12Z is 296 K at 950 mb. The top of the inversion then rises from 12Z to 17Z to 900 mb with a maximum temperature starting at 294 K and ending at 291 K. The top of the inversion once again lowers from 17Z to the end of the period to a level of 925 mb and a maximum temperature of 294 K. A very strong vertical temperature gradient is present throughout the entire period through the marine inversion; however, a weakening is noted when the inversion rises around 17Z. The thermal structure above 800 mb is rather smooth with only a few small scale features present like the small cold pocket at 825 mb at 03Z.

The main feature in the moisture timesections on 10 May (Fig. 11c) remains the surface moist layer. The surface moisture layer is once again well defined with its strongest gradient at the base of the inversion throughout the entire period. The surface moist layer rises with the base of the inversion from 12Z to 17Z. Unlike 9 May, no small scale features are detected during the day. As a result, there is a smooth transition from the moist surface to the dry mid-troposphere. There is a gradual moistening of the surface layer through the whole day, reaching its peak at 17Z.

4. GB-HIS Timesections (10 May 92)

The GB-HIS successfully depicted the behavior of the marine inversion on May 10th (Fig. 11b). In the beginning of

the day (00Z to 06Z) the maximum temperature at the top of the inversion is analyzed to be 297 K at a height of 940 mb. From 06Z to 14Z the maximum temperature above the inversion drops to 294 K. From 14Z to the end of the period the top of the inversion gradually rises to 910 mb with the maximum temperature decreasing to 290 K. Of particular note is the GB-HIS detection of the change in the marine inversion after 14Z.

The GB-HIS data successfully indicate a strong surface layer moisture gradient corresponding to the marine inversion through the entire day (Fig. 11d). Slow drying occurs above the base of the inversion throughout most of the day, except after 17Z where very rapid drying occurs. The moisture gradient shows a smooth decrease from the surface to the base of the inversion. No small scale features are detected during the day. The general pattern of the GB-HIS moisture analysis agrees well with the rawinsondes except for the drying above 900 mb at the end of the period.

B. 1991 CRUISE

1. Rawinsonde Timesections (8 May 91)

The rawinsonde temperature timesection for 8 May 91 (Fig. 12a) displays the cooling in the boundary layer as a cold front approaches the central California coast. A

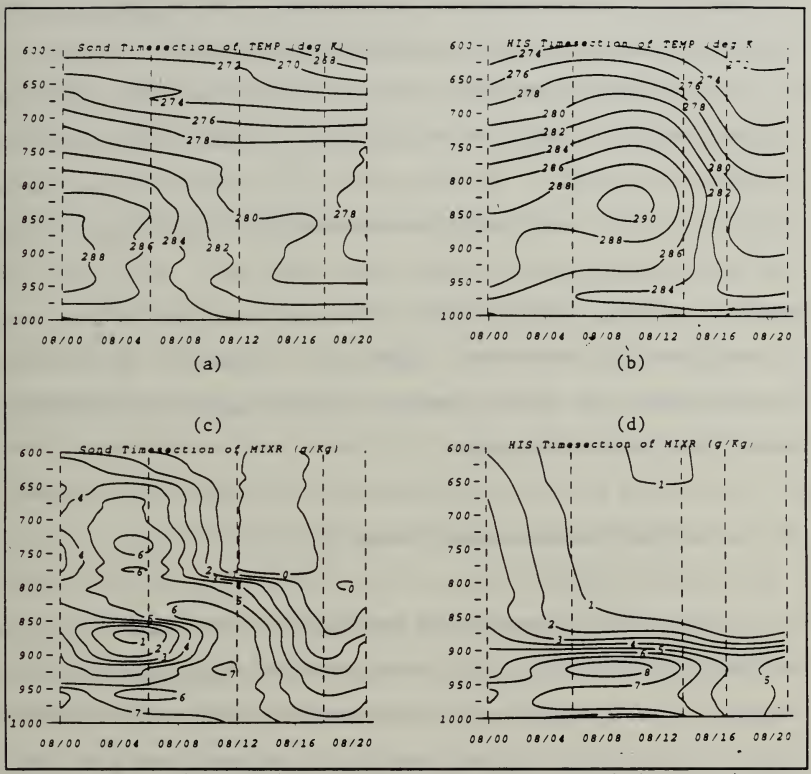

Figure 12: Timesections of temperature and mixing ratio for the rawinsonde, (a) and (c), and the GB-HIS, (b) and (d), over the period of 910508/0000 GMT to 910508/2400 GMT. Mixing ratio is in g/Kg and temperature is in °K.

noticeable cooling is depicted after the frontal passage (14Z) to the end of the day. A distinct change from the stable air ahead of the front to less stable air after the front is detected in the temperature timesection. From 800 mb to 600 mb the atmosphere shows a small cooling trend.

The rawinsonde mixing ratio timesection (Fig. 12c) is quite complex. Early in the period, several moist and dry layers are evident. In particular, the 08/0600Z rawinsonde depicts a moist surface layer below 900 mb, a dry layer at 880 mb, and another moist layer above 800 mb. After the 14Z frontal passage, there is rapid cooling an drying in the lower troposphere below 800 mb. Immediately above 800 mb there is a large amount of drying possibly indicating strong subsidence after the frontal passage.

2. GB-HIS Timesections (8 May 91)

The GB-HIS temperature timesection (Fig. 12b) indicates a lifting of the initial inversion with evolution of a warm anomaly at 09Z centered 850 mb with a maximum temperature of 291 K. After 12Z, a strong cooling is evident from just above the surface layer through the low troposphere. By 17Z the low level inversion is gone and the temperature decreases with height from the surface to 600 mb. Although the GB-HIS measurements indicate a lifting and destruction of the marine

inversion followed by cooling, there are marked differences between rawinsondes and GB-HIS analyses.

The dominant feature in the GB-HIS timesection of mixing ratio (Fig. 12d) is the constant height and strength of a moisture layer with the marine inversion. Rapid drying is evident above 875 mb after 06Z. The GB-HIS timesection also depicts some drying in the PBL after the frontal passage.

3. Rawinsonde Timesections (9 May 91)

Throughout the 9 May and into the 10 May, a very noticeable feature in the rawinsonde timesection of temperature (Fig. 13a) is the well-mixed PBL (below 875 mb) which exhibits a near adiabatic lapse rate after the frontal passage. The upper level passage of the cold front after 00Z is also quite evident by the strong cooling above 825 mb. Above 800 mb the coldest air is found between 06Z and 12Z.

The rawinsonde moisture data shows dry air above 800 mb with mixing ratio increasing to 4 to 5 g/Kg near the surface. There is no major changes during the day.

4. GB-HIS Timesections (9 May 91)

The most noticeable feature on the GB-HIS temperature timesection (Fig. 13b) is the even spaced lower PBL isotherms (below 875 mb) throughout the whole day. The upper level

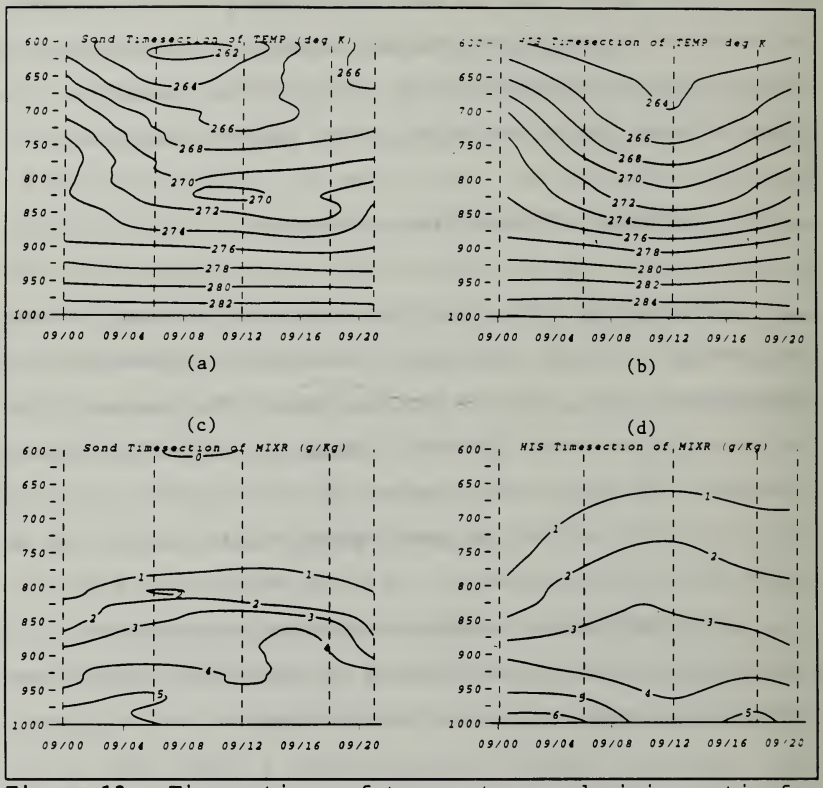

Figure 13: Timesections of temperature and mixing ratio for the rawinsonde, (a) and (c), and the GB-HIS, (b) and (d), over the period 910509/0000 GMT to 910509/2400 GMT. Mixing ratio is in g/Kg and temperature is in °K.

cooling is also evident on this timesection, beginning around 00Z. The strong cooling of the upper level is in general agreement with the observed data.

The GB-HIS timesection of mixing ratio (Fig. 13d) shows a general decrease of moisture from the surface to 600 mb. There are no distinct features on this timesection due to the well modified PBL occurring after the cold frontal passage. The GB-HIS moisture values are somewhat higher near the surface and in the upper levels (above 800 mb).

C. STRENGTHS AND WEAKNESSES OF RAWINSONDE vs. GB-HIS

1. 1992 Point Sur Cruise

In comparison to the rawinsonde results, the GB-HIS retrievals show both strengths and weaknesses in measuring lower tropospheric changes. The most obvious strength of the GB-HIS profiles is the detection of a marine temperature inversion throughout the entire cruise (Figs. 14a and b). Secondly, the GB-HIS detects fluctuations in the inversion height and strength such as the inversion layer change on the 10th (14Z to 17Z) (Fig. 11b). The GB-HIS also successfully depicts the relative strength of the marine inversion, remaining within 2-3 K of the rawinsonde for the inversion top on both days. On both days, relative features in the vertical

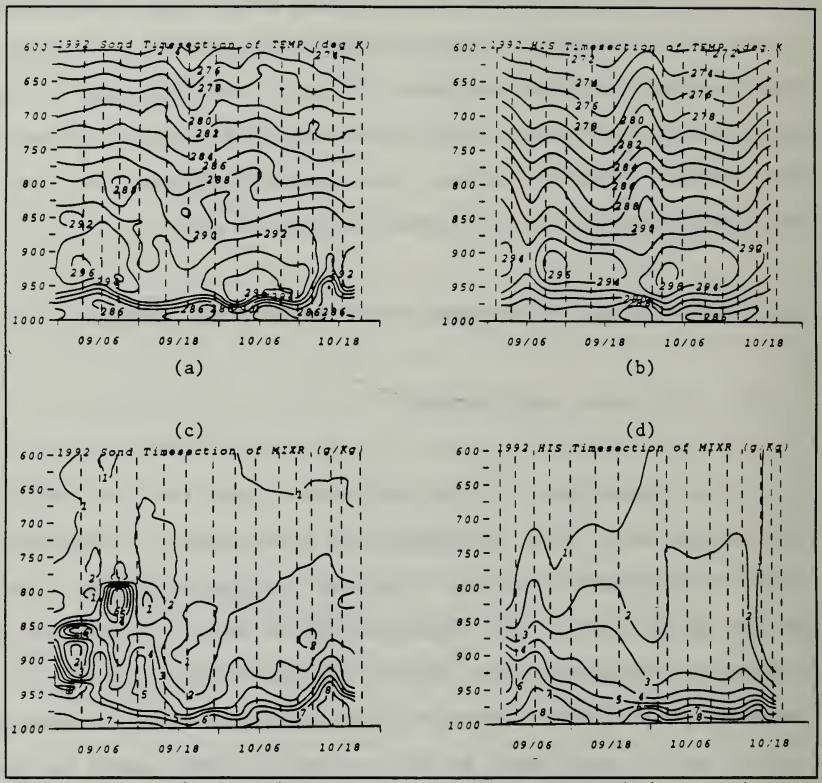

Figure 14: Timesections for temperature and mixing ratio for the rawinsonde, (a) and (c), and the GB-HIS, (b) and (d), over the period of 920509/0000 GMT to 920510/2400 GMT. Mixing ratio is in g/Kg and temperature is in °K.

temperature structure above 800 mb are depicted well by the GB-HIS.

The surface moist layer is also depicted well by the GB-HIS on both days (Fig. 11d). Long term (> 6 hrs) moisture changes were handled well on the 9th as the GB-HIS detected the gradual decrease in moisture through the day (Fig. 10d). Although moisture fluctuations on the 10th are not portrayed as well, the height of the low level moist layer is. Small scale moist and dry layers are not totally missed, but are indicated to by ridging and troughing in the contouring. This can be seen on Fig. 11d, which shows ridging in the boundary layer (around 17Z) in conjunction with large moistening in Fig. 11c, or troughing on Fig. 10d in conjunction with rapid drying above the base of 850 mb on Fig. 10c at 00Z to 03Z. Although this capability may not be substantial, the GB-HIS results show there is some skill in detecting these changes.

The most notable weaknesses of the GB-HIS retrievals concern missing details of the moisture profiles. Obvious of these weaknesses is the inability of the GB-HIS to resolve fine scale (< 50 mb) moisture features. This is best depicted on the 9th between 00Z and 03Z (Figs. 10c and d), where sharp moist and dry layers are found all within in 100 mb and are not present on the GB-HIS timesection. Other weaknesses include 1) a weaker moisture gradient from the surface to base of the inversion, 2) a continuous and weaker temperature gradient from the surface to the top of the inversion, 3) a

tendency to analyze the top of the inversion too high, and 4) a overestimation of the moisture near the surface.

2. 1991 Point Sur Cruise

The most notable strength of the GB-HIS during 1991 Point Sur cruise is the ambient temperature throughout the timeframe was within 3 °C of rawinsonde data (Figs. 15a and b). There is also very good agreement in the vertical temperature and moisture structure throughout the low troposphere on the 9th of May (Fig. 13). The GB-HIS also displayed the general observed trend of cooling as the cold front approached and passed. The GB-HIS moisture timesection does display a marine layer moisture gradient up to 900 mb prior to the frontal passage which is in good agreement with the rawinsonde placement (Fig. 12c and d). At 08/13Z the GB-HIS moisture timesection captured the frontal drying from the surface to 925 mb, and the general drying trend in the mid-troposphere that followed compared to the rawinsondes.

The GB-HIS moisture retrievals were less successful in 1992 cruise. In particular, specific moisture layers are not captured and the pronounced drying on 8 May was analyzed to be too dry and too early (Fig. 15). Although, the general temperature changes for the 1991 cruise are resolved by the GB-HIS, a number of the details in thermal structure are not well described. On 8 May, the behavior of the marine

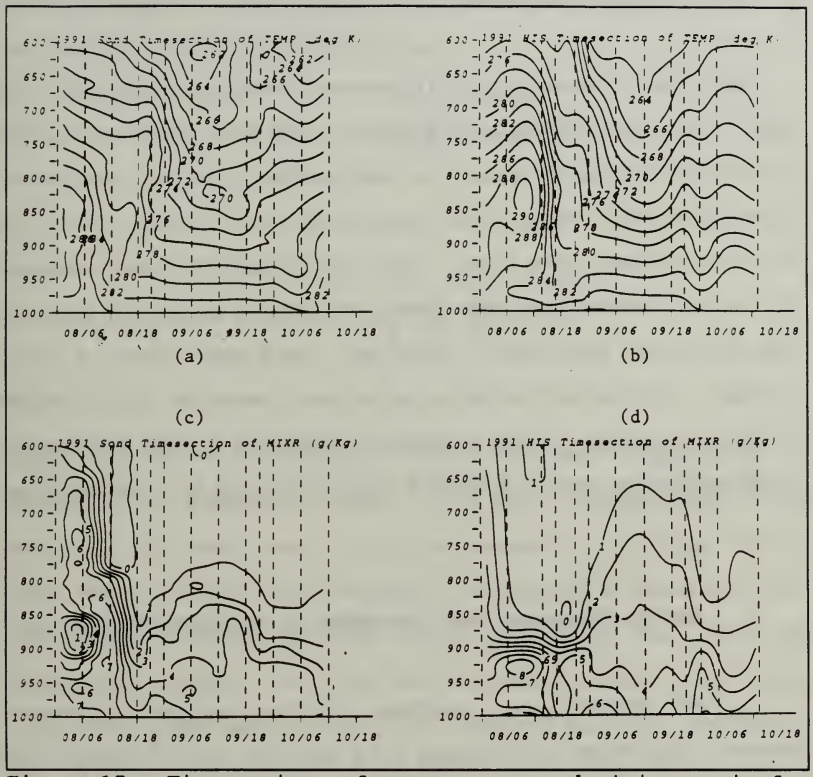

Figure 15: Timesections of temperature and mixing ratio for the rawinsonde, (a) and (c), and the HIS, (b) and (d), over the period 910508/0000 GMT to 910510/1200 GMT. Mixing ratio is in g/Kg and temperature is in °K.

inversion and its collapse as the front approached is depicted differently by the GB-HIS retrievals.

D. Statistical Analyses

Root Mean Square (rms) Difference, Standard Deviation (std dev), Bias, and Explained Variance (exp var) were calculated on the GB-HIS data using the rawinsonde data for reference. Statistics were calculated every 5 mb from 1000 mb up to 700 mb and averaged over time. The rms difference when compared to the atmospheric std dev describes the existence of skill in the retrieval algorithm. When rms < std dev, there is skill present. Explained variance provides a measure of the degree of skill present. Bias provides a measure of the systematic differences between the GB-HIS retrievals and the rawinsondes.

1. RMS Differences and Atmospheric Standard Deviation

RMS values are a measure of the average difference between the known rawinsonde data and the calculated GB-HIS data at the same level. The smaller the rms difference, the more accurate is the GB-HIS retrieval algorithm. The atmospheric std dev is a measure of the atmospheric changes from the time of the guess profile (used to initialize the retrieval algorithm) to the time of a subsequent rawinsonde

profile. A small std dev indicates small atmospheric changes at that level. Thus, the smaller the std dev, the more difficult it becomes to establish skill since little change occurs from the first guess. The rms and atmospheric std dev values are calculated as follows:

$$rms = \sqrt{\frac{1}{n}\sum_{i=1}^{n}(X_h - X_s)_i^2} \qquad (1)$$

$$std\ dev = \sqrt{\frac{1}{n-1}\sum_{i=1}^{n}(X_s - \overline{X_s})_i^2}$$

where X_s is the rawinsonde value (either temperature or dewpoint) at a specific level, X_h is the corresponding GB-HIS value at the same level, n is the number of soundings in the data set, and $\overline{X}_s$ is the retrieval algorithm's guess profile. The guess profile in this study is always the 0000 GMT rawinsonde profile for each day of each cruise. The above quantities, rms and std dev, are computed for each individual day of the cruise (n = 4 to 8), the entirety of a single year's cruise (n = 10 or 14), and the two cruises combined into one data set (n = 24). The guess profiles are not included into the value of n.

a. 1992 Point Sur Cruise

Results from the 1992 cruise show that all rms temperature differences for both days remained under 3.5 K for all levels (Figs. 16 and 17). Skill was realized in the lowest level from approximately 940 mb to the surface on both days, while there was sporadic evidence of skill at the remaining higher levels. Similarly, rms temperature differences are smaller for lower levels indicating better ability to resolve the lower planetary boundary layer (PBL). In fact, the GB-HIS measured the average marine inversion strength at a approximately 950 mb throughout the 1992 cruise to within 2.5 K (Fig. 18).

The rms dewpoint differences are large (< 15 K) on the 10th (Fig. 20) due to higher frequency of clouds in the GB-HIS field of view, with only slightly smaller values on the 9th (< 9.5 K) (Fig. 19). Results show skill in the lowest level on both days and continues to show skill throughout the low troposphere on the 9th, while the 10th shows no skill above this level. The two days combined (Fig. 21) show a relative maximum in rms dewpoint differences at the top of the marine inversion, then less rms differences above it, indicating difficulty in resolving the moisture gradient of the marine inversion.

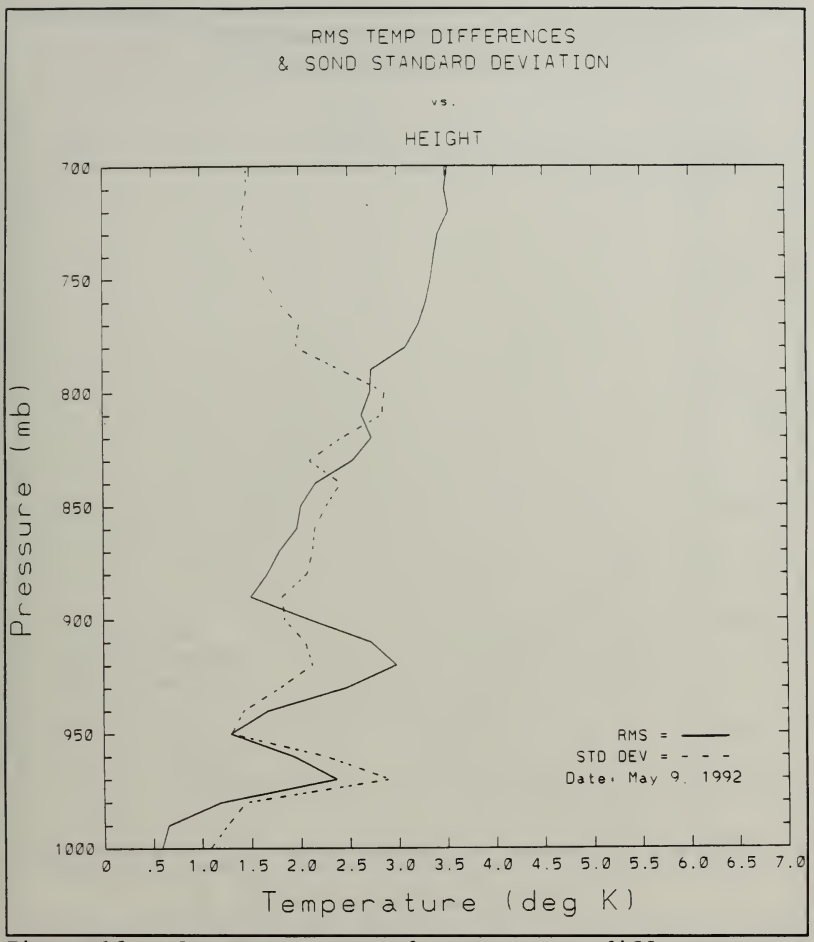

Figure 16: Root mean squared temperature differences are compared to atmospheric standard deviation for 9 May 92. Skill is noted when rms is less than std dev.

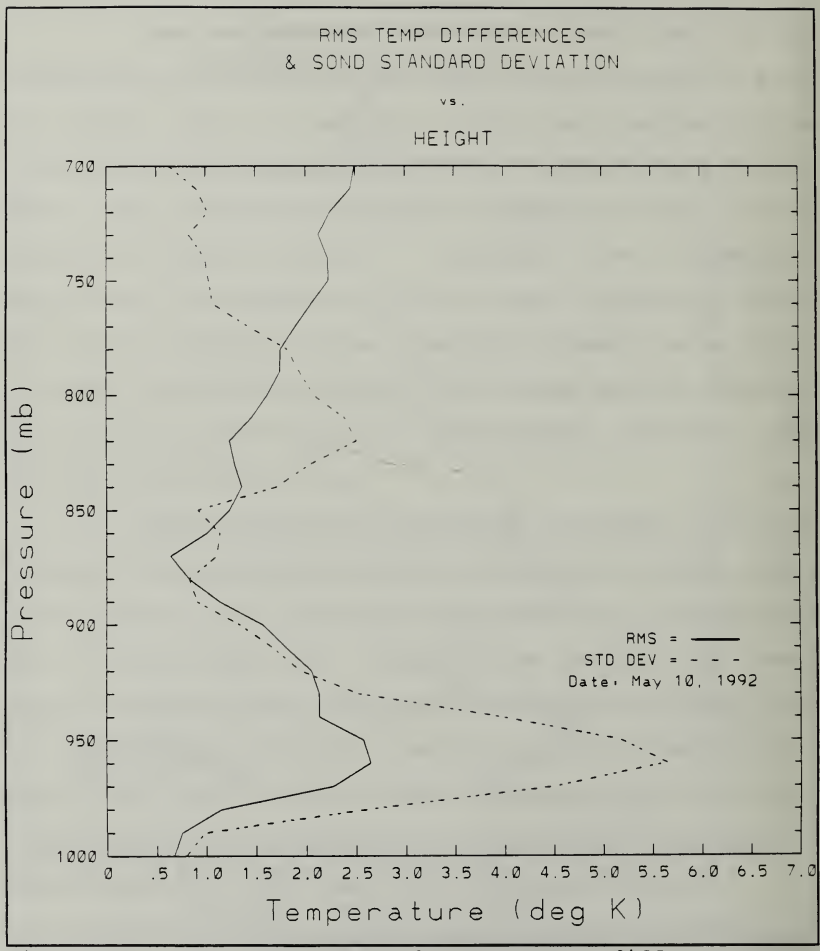

Figure 17: Root mean squared temperature differences are compared to atmospheric standard deviation for 10 May 92. Skill is noted when the rms is less than the std dev.

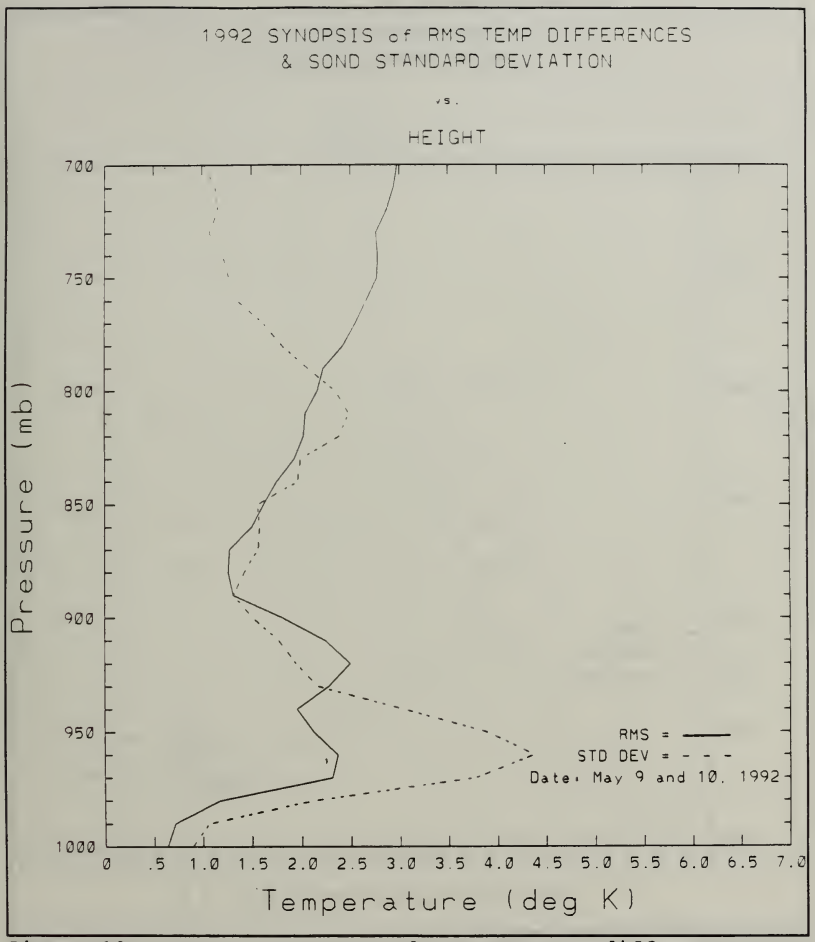

Figure 18: Root mean squared temperature differences are compared to atmospheric standard deviation for the 1992 cruise. Skill is noted when rms is less than std dev.

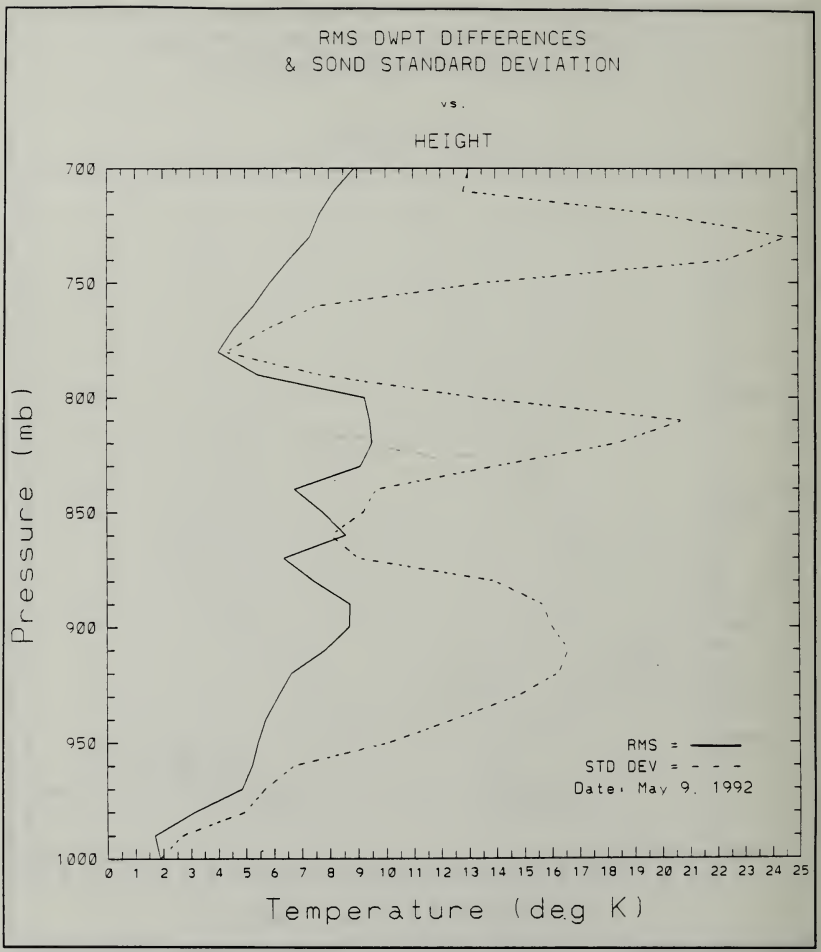

Figure 19: Root mean squared dewpoint differences are compared to atmospheric standard deviation for 9 May 92. Skill is noted when rms is less than std dev.

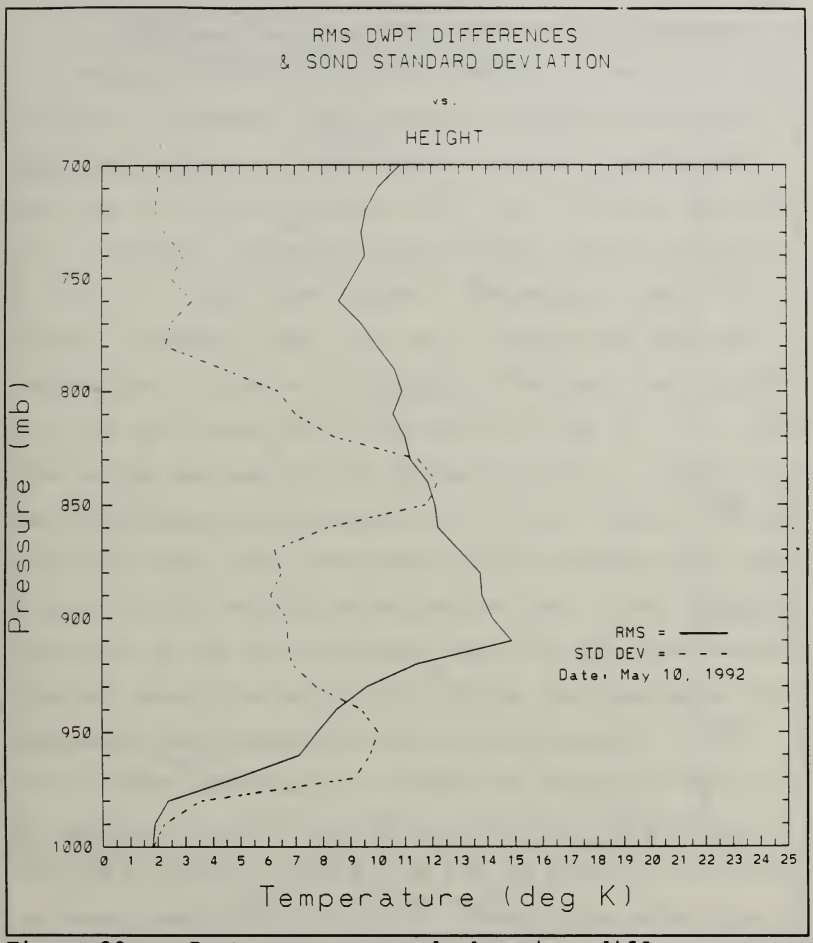

Figure 20: Root mean squared dewpoint differences are compared to atmospheric standard deviation for 10 May 92. Skill is noted when rms is less than std dev.

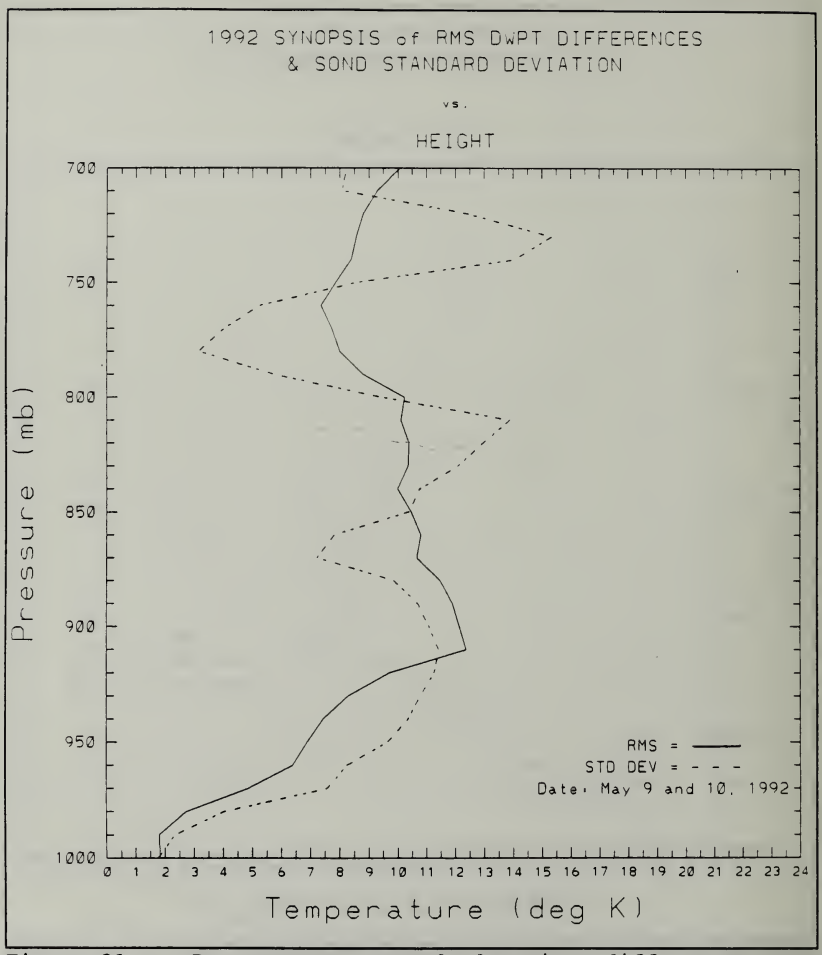

Figure 21: Root mean squared dewpoint differences are compared to atmospheric standard deviation for the 1992 cruise. Skill is noted when rms is less than std dev.

b. 1991 Point Sur Cruise

Results show that rms temperature differences for all levels on the 8th and the 9th remained under 5.0 K (Figs. 22 and 23); however, when averaged together to include the 10th, rms temperature differences improved significantly to less than 3.5 K for all levels (Fig. 24). The best rms values are, in general, noted near the surface, ranging between 1.0 K and 1.5 K, and then steadily decreasing upward with a maximum generally near 900 mb. Skill was realized on temperature profiles at virtually all levels on the 8th (Fig. 22), but only above 880 mb on the 9th (Fig. 23). A closer look at the rms and std dev values on the 9th, reveals that rms values remain respectably low (< 3.0 K); however, there is also very small std dev values which indicate only small changes in the atmosphere during the day. The "no skill" influence of the 9th is noted when all data are averaged together showing no skill up to 990 mb, but displaying skill throughout the remainder of the low troposphere.

The rms dewpoint differences are quite small near the surface (below 970 mb) on the 8th with values below 1.5 K (Fig. 25); however, above 970 mb the rms dewpoint differences increase dramatically to 21.0 K. These large departures are due mostly to the problem the GB-HIS had detecting the moisture changes caused by the strong subsidence associated with the front. Even though these rms values became large,

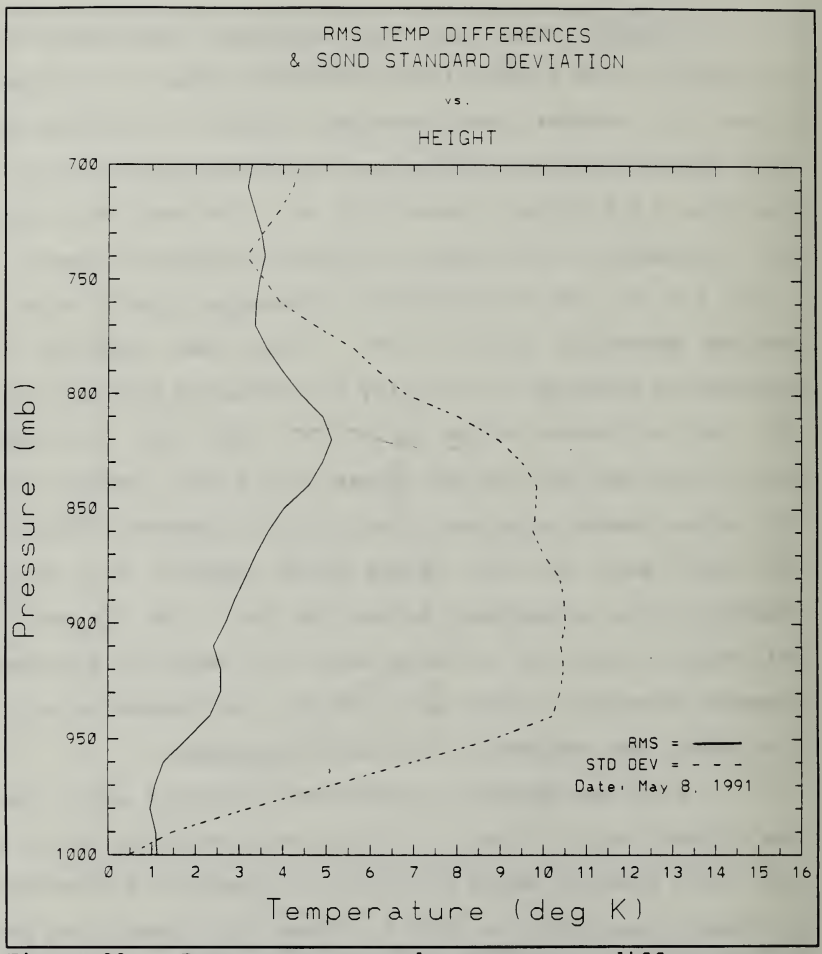

Figure 22: Root mean squared temperature differences are compared to atmospheric standard deviation for 8 May 91. Skill is noted when rms is less than std dev.

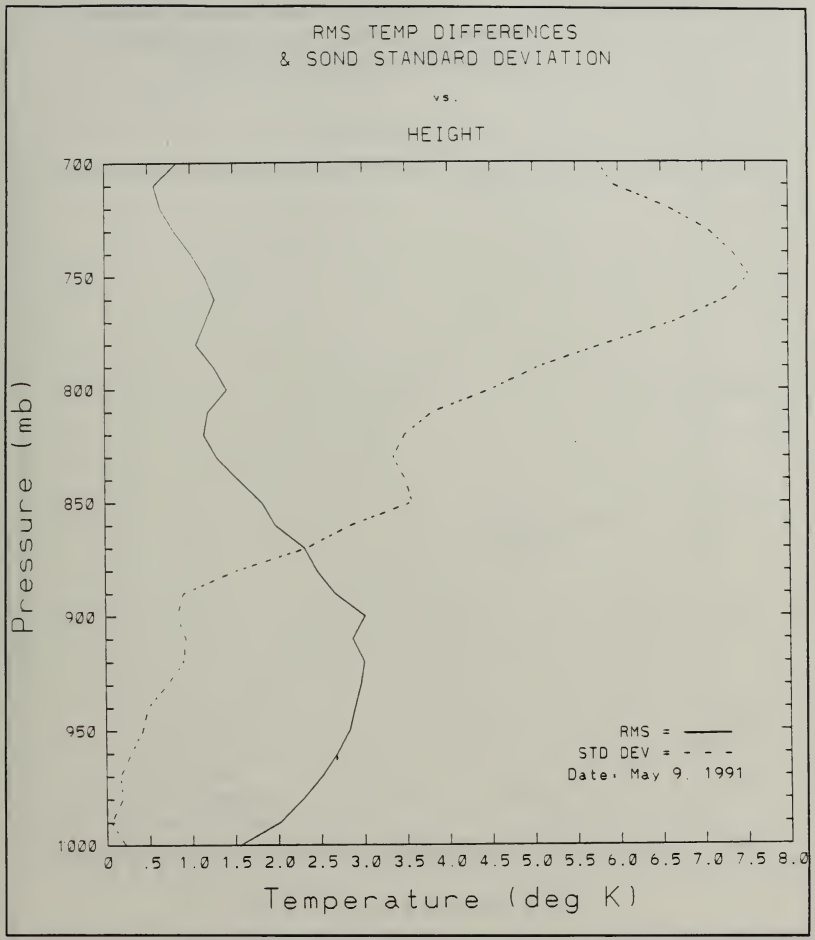

Figure 23: Root mean squared temperature differences are compared to atmospheric standard deviation for 9 May 91. Skill is noted when rms is less than std dev.

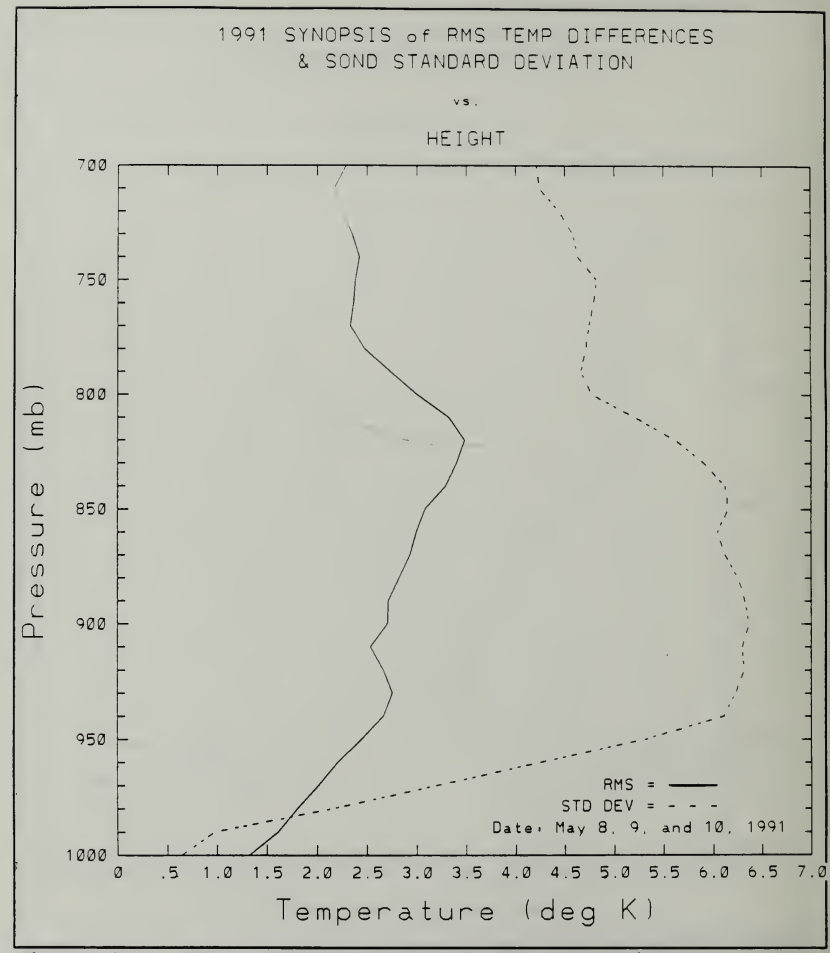

Figure 24: Root mean squared temperature differences are compared to atmospheric standard deviation for the 1991 cruise. Skill is noted when rms is less than std dev.

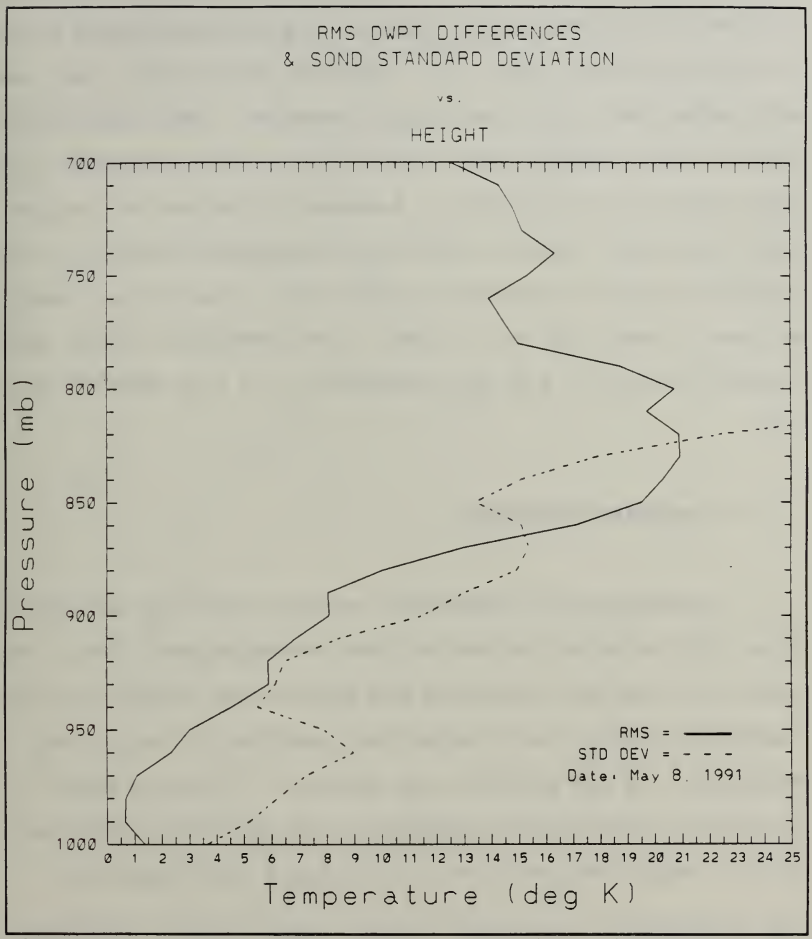

Figure 25: Root mean squared dewpoint differences are compared to atmospheric standard deviation for 8 May 91. Skill is noted when rms is less than std dev.

still skill was achieved from the surface to approximately 860 mb and also above 820 mb. The rms dewpoint differences noted on the 9th were much better than on the 8th with values below 3 K up to 880 mb (Fig. 26). This is due to the clear and well-mixed PBL after the frontal passage. RMS values above 880 mb also became large, up to 18.0 K, but increased less with height than on the 8th. Because the PBL was well-mixed, there was also a smaller amount of atmospheric variation with height and time; consequently, skill was achieved just barely at most levels up to 770 mb. RMS dewpoint values grew steadily from 1.5 K at the surface to 6.0 K at 890 mb (Fig. 27).

2. Explained Variance

Statistics for explained variance are also calculated from 1000 mb up to 700 mb and then averaged over time. The statistic "exp var" indicates how much of the variability from the guess profile, with which the algorithm is initialized, a subsequent GB-HIS profile can explain. In other words, it provides a quantitative measure of the retrieval algorithm's skill. Explained variance is calculated from Equation 2,

$$\text{exp } var = 1 - \frac{(RMS)^2}{\sigma_s} \qquad (2)$$

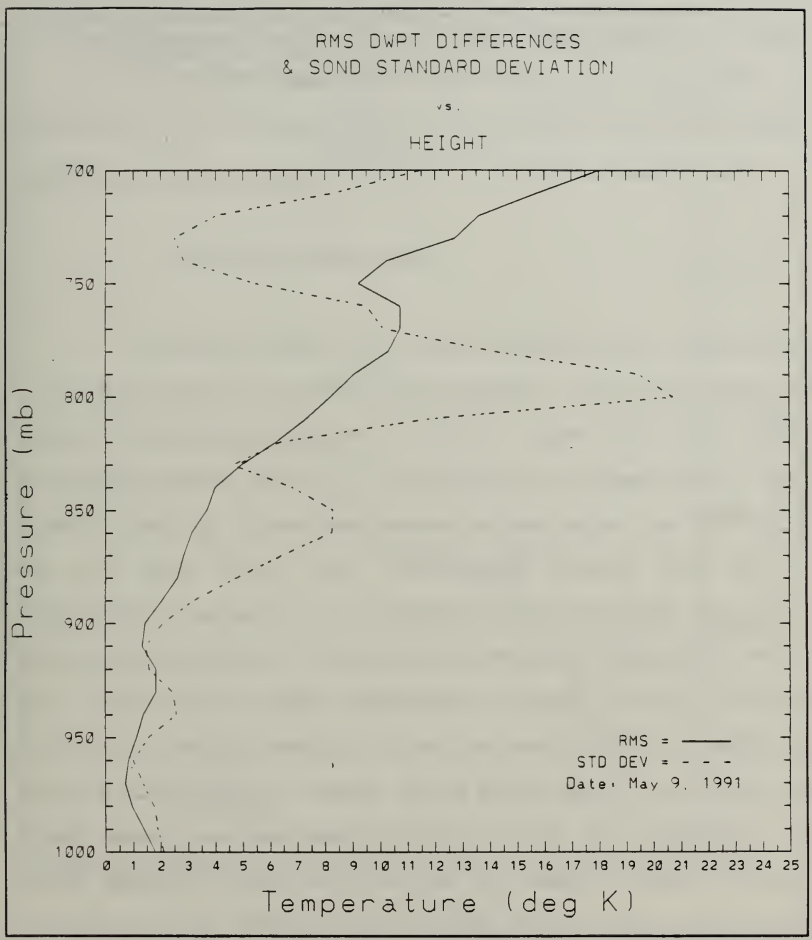

Figure 26: Root mean squared dewpoint differences are compared to atmospheric standard deviation for 9 May 91. Skill is noted when rms is less than std dev.

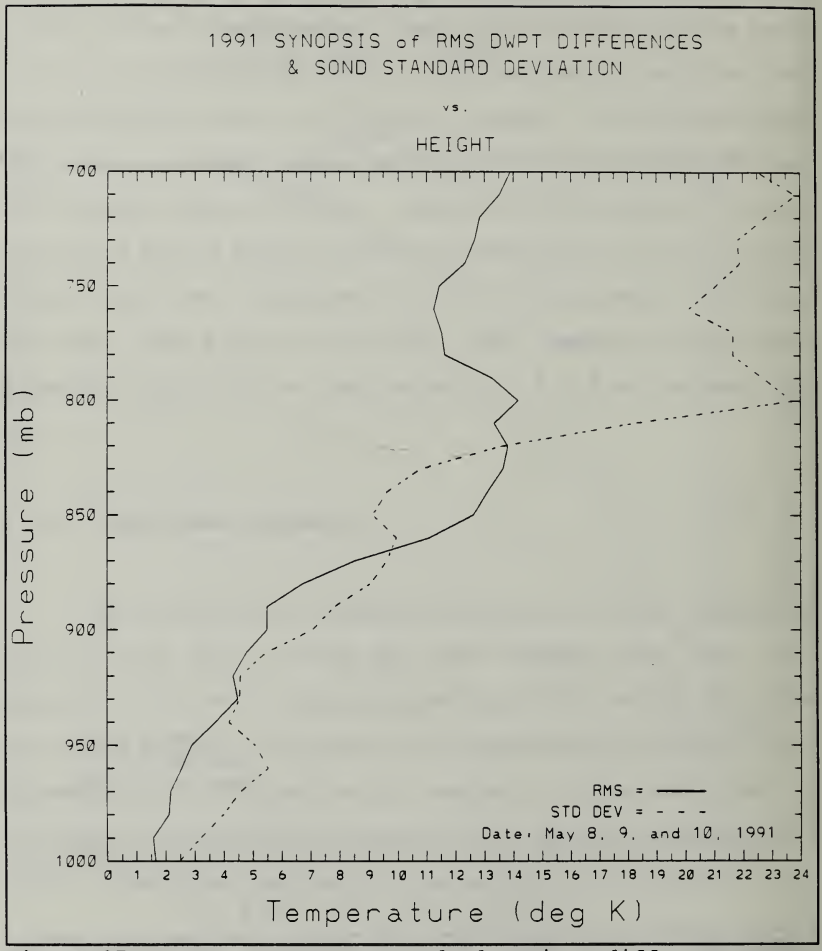

Figure 27: Root mean squared dewpoint differences are compared to atmospheric standard deviation for the 1991 cruise. Skill is noted when rms is less than std dev.

where RMS is the root mean square difference at a specific level and σ_s is the atmospheric variance at a specific point in time measured from the time of the guess profile. A value of "1" or "100%" means all the atmospheric variance is explained by the corresponding GB-HIS profile up to that point in time.

a. 1992 Point Sur Cruise

General results of this statistic for temperature retrievals shows, for both days combined, the lowest level has the most variance explained or skill. Less skill is attained at higher levels (Fig. 30). Good skill was realized on both 9 and 10 May up to marine inversion tops with the best skill on the 10th (Fig. 29), explaining nearly 80% of the atmospheric variance. On average for both days, the lower level skill peaked at 70% explained variance, the mid-level at 35%, and with no skill observed at higher levels. On the other hand, GB-HIS dewpoint profiles had difficulty capturing small scale moisture layers where small gaps of no skill are found throughout the low troposphere (Fig. 28). However, the skill remained quite high on the 9th despite those no skill layers, but the intermittent clouds on the 10th limited any skill above the marine inversion. Overall, the dewpoint profiles also did moderately well up to the top of the marine inversion (50 - 60% variance explained). They showed some

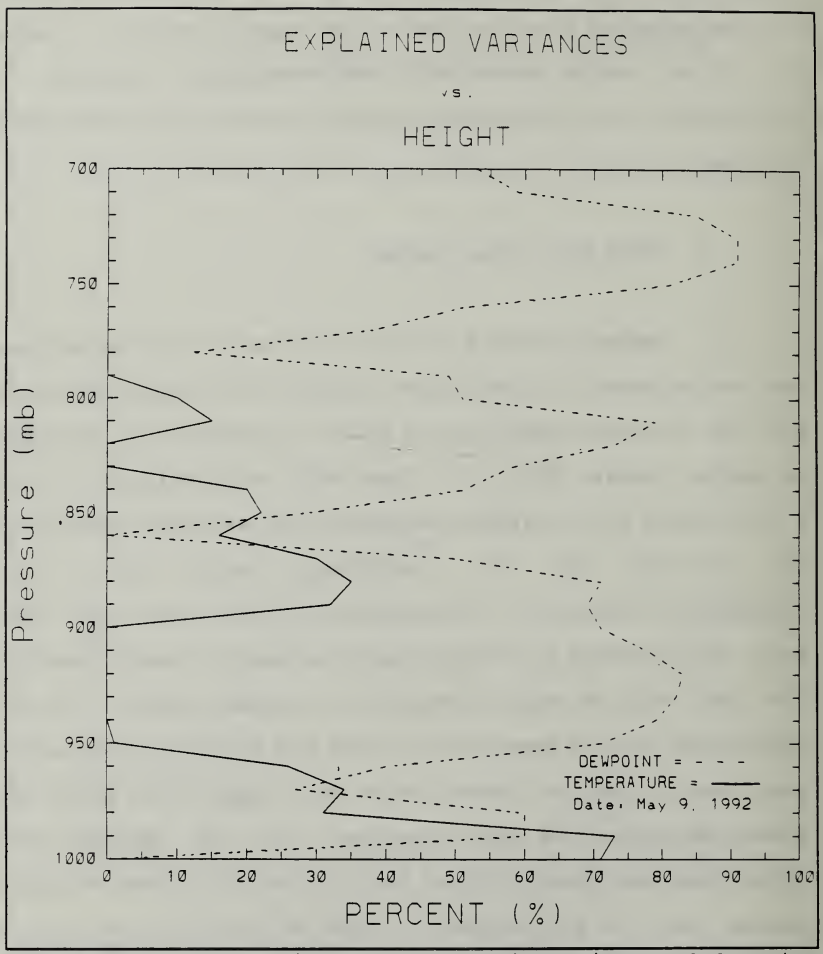

Figure 28: The quantity of atmospheric variance of dewpoint and temperature profiles explained by the HIS. Variance is based on the 09/0000 GMT rawinsonde profile.

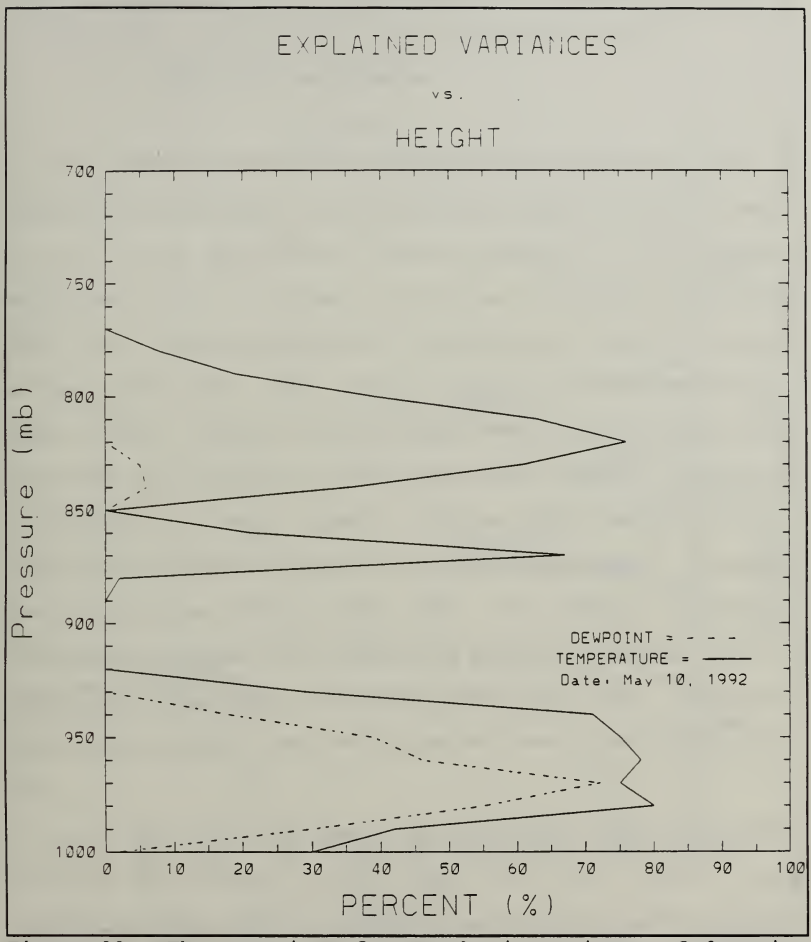

Figure 29: The quantity of atmospheric variance of dewpoint and temperature profiles explained by the HIS. Variance is based on the 10/0000 GMT rawinsonde profile.

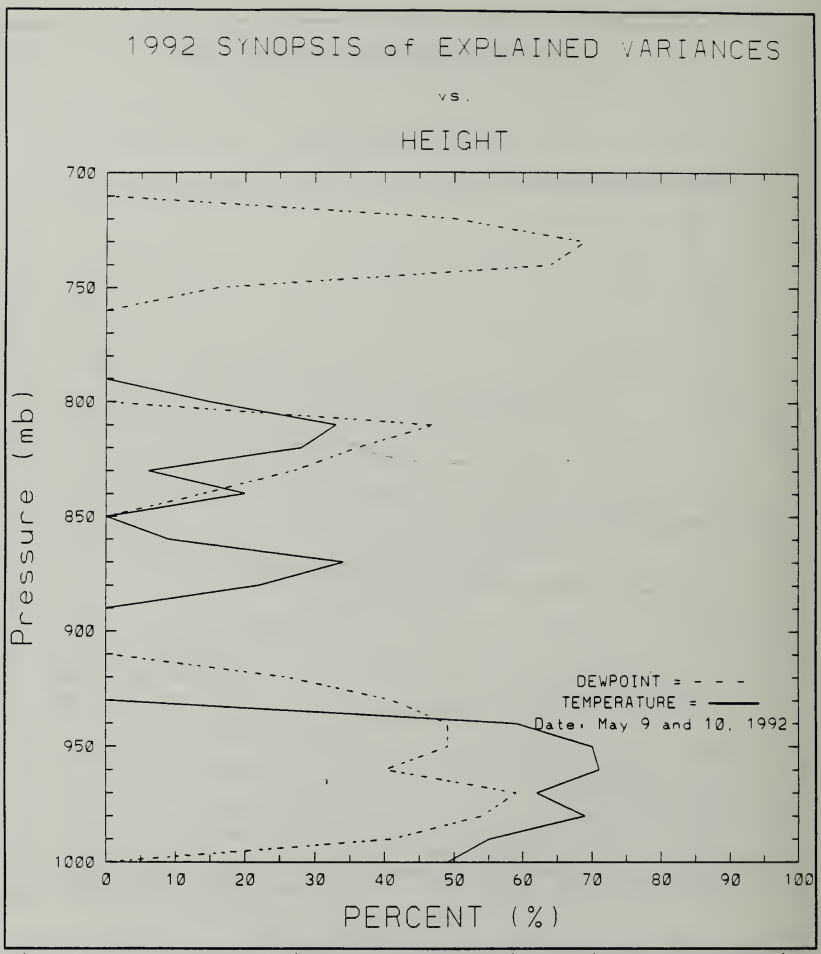

Figure 30: The quantity of atmospheric variance of dewpoint and temperature profiles explained by the HIS. Variance is based on the 0000 GMT rawinsonde profiles for each of the days of the cruise.

skill in the mid-levels (35 - 45% variance explained), and explained nearly 70% of the atmospheric variance above 750 mb.

b. 1991 Point Sur Cruise

The results of explained variance for the temperature profiles on the 8th show a large amount of skill in the low to mid-PBL with 80% or greater of the variance explained (Fig. 31). Even up to 770 mb, the skill was greater than 50%. This is excellent, considering a cold front passed through this day. The 9th was equally as skillful in the upper levels. Recall that the small amount of atmospheric std dev from the surface to the mid-levels greatly limits the skill in the lowest layers. Above this layer, skill is measured at greater than 50% variance explained, exceeding even 80% above 840 mb (Fig. 32). In general, the skill displayed by the GB-HIS temperature profiles averaged over the three day timeframe of the cruise is very successful, explaining greater than 60% of the variance above 970 mb (Fig. 33).

As for the moisture profiles, the 1991 skill profiles are similar to the 1992 Point Sur cruise. Large amounts of skill were attained on both the 8th (Fig. 31) and the 9th (Fig. 32) below 950 mb explaining more than 50% of the variance through most of the layer and peaking at 99% on the 9th at 980 mb. A mid-level peak in skill is also noticed on

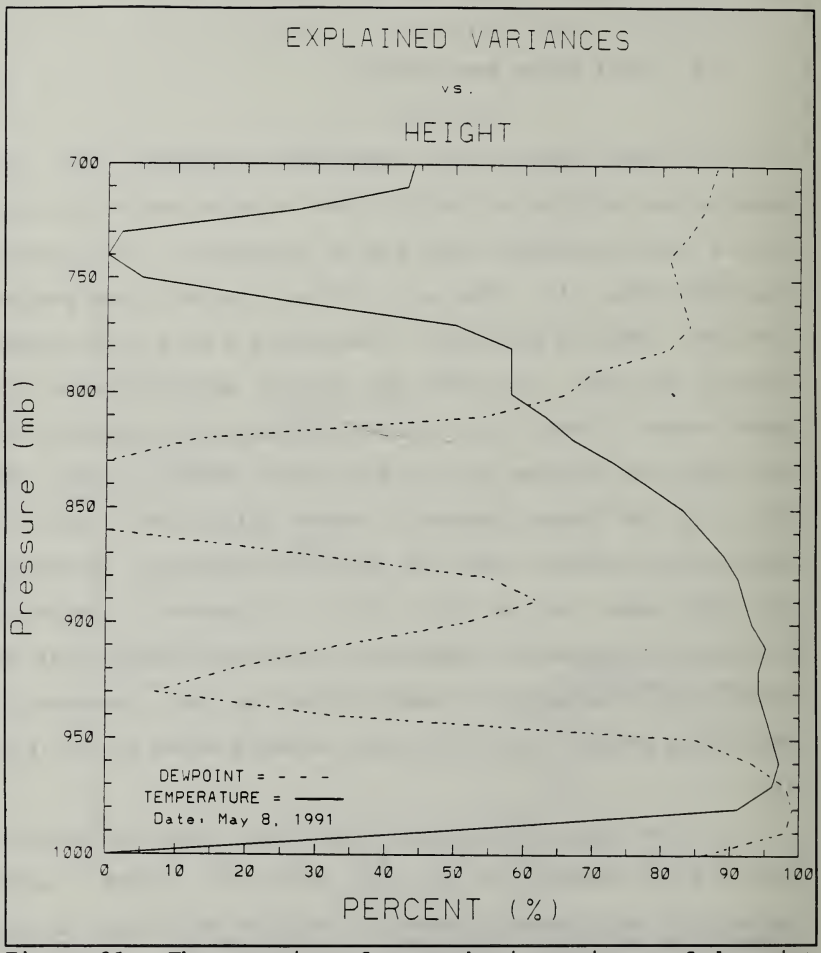

Figure 31: The quantity of atmospheric variance of dewpoint and temperature profiles explained by the HIS. Variance is based on the 08/0000 GMT rawinsonde profile.

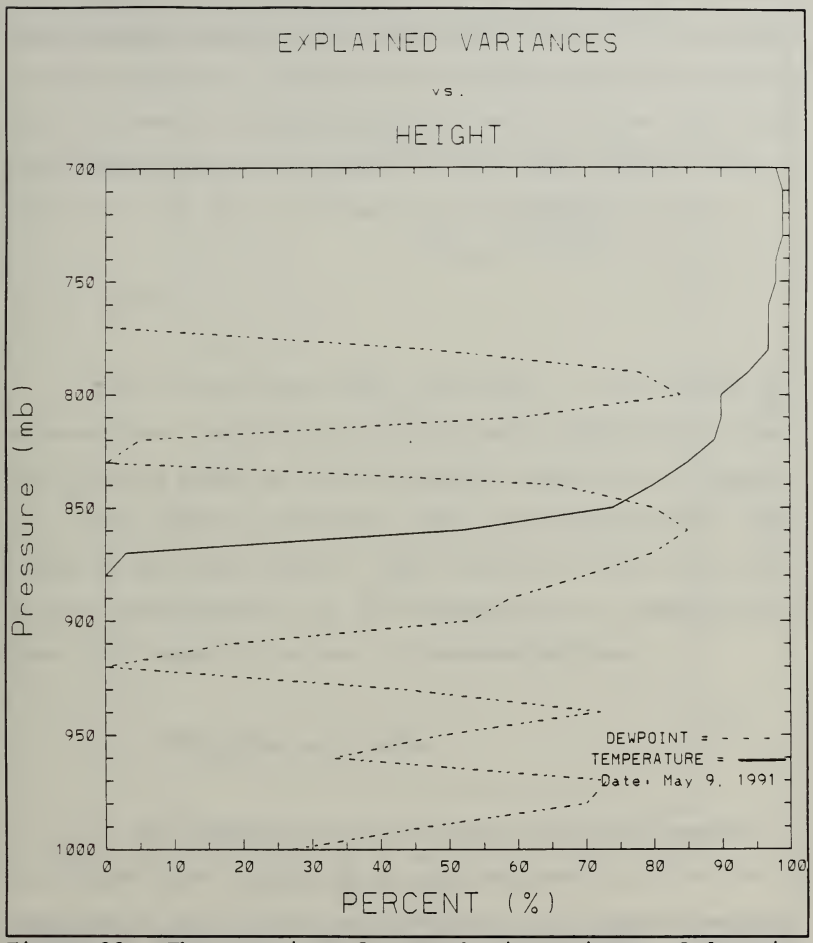

Figure 32: The quantity of atmospheric variance of dewpoint and temperature profiles explained by the GB-HIS. Variance is based on the 09/0000 GMT rawinsonde profile.

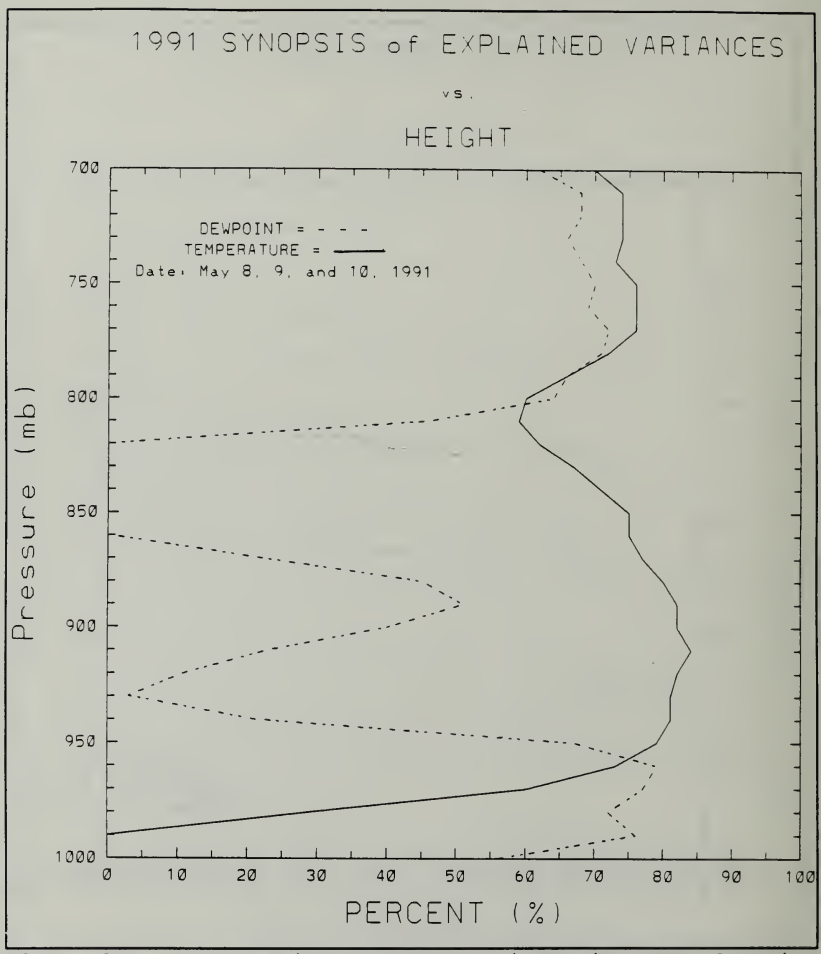

Figure 33: The quantity of atmospheric variance of dewpoint and temperature profiles explained by the GB-HIS. Variance is based on the 0000 GMT rawinsonde profiles for each of the days of the cruise.

both days, centered around 870 mb, explaining more than 60% of the variance. This spike in skill is much larger than the one which occurred during the 1992 cruise. Unique to this cruise is the existence of skill in the moisture profiles above 830 mb. The overall synopsis of skill over the three days (Fig. 33), demonstrates the average of the same general vertical pattern of the skill displayed on the 8th and the 9th.

3. Bias

Bias values are also calculated at each level and averaged over time for both dewpoint and temperature profiles. The bias was based on the rawinsonde temperature or dewpoint at a level being subtracted from the corresponding GB-HIS values at the same level. Thus, positive values indicate a GB-HIS overestimation of the temperature or dewpoint at a level, and negative values, an underestimation.

a. 1992 Point Sur Cruise

The temperature bias on both the 9th and the 10th in the lowest level indicates an underestimation of the actual temperature for the marine inversion top (Figs. 34 and 35). Compensating for that negative bias, both days also show a 1.0 - 1.5 K positive bias above the marine inversion. Thus, the retrieval algorithm depicts a higher marine inversion as seen

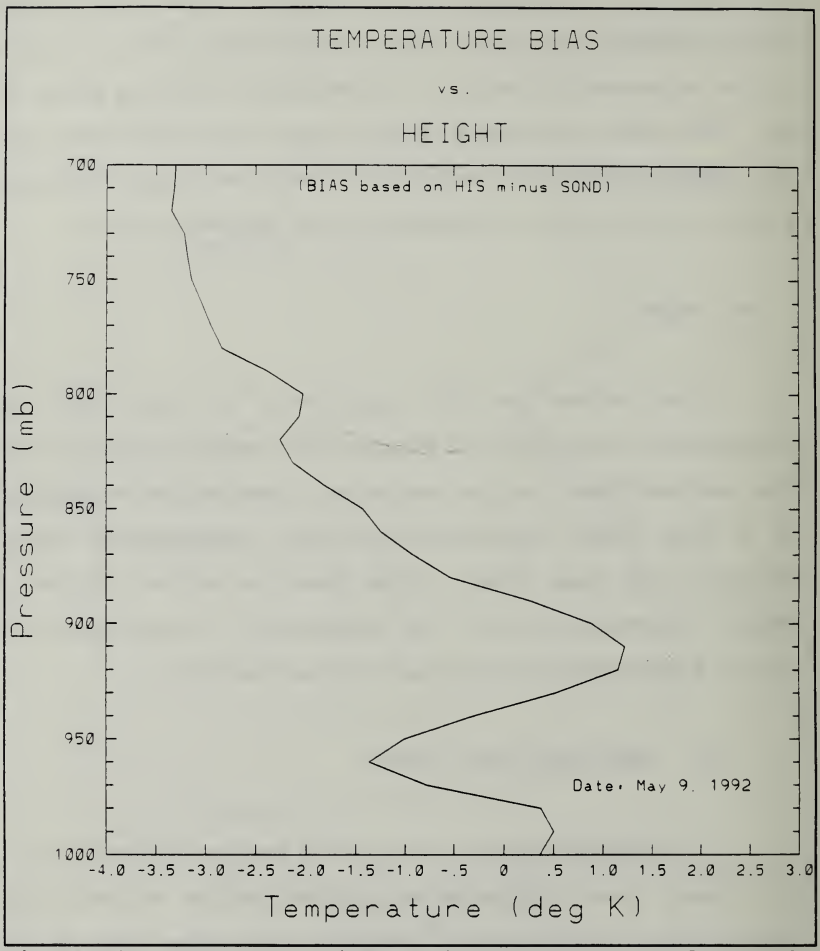

Figure 34: Temperature bias profile based on the value of the HIS minus the value of the rawinsonde at same level. A positive bias indicates an overestimation and a negative bias an underestimation of temperature.

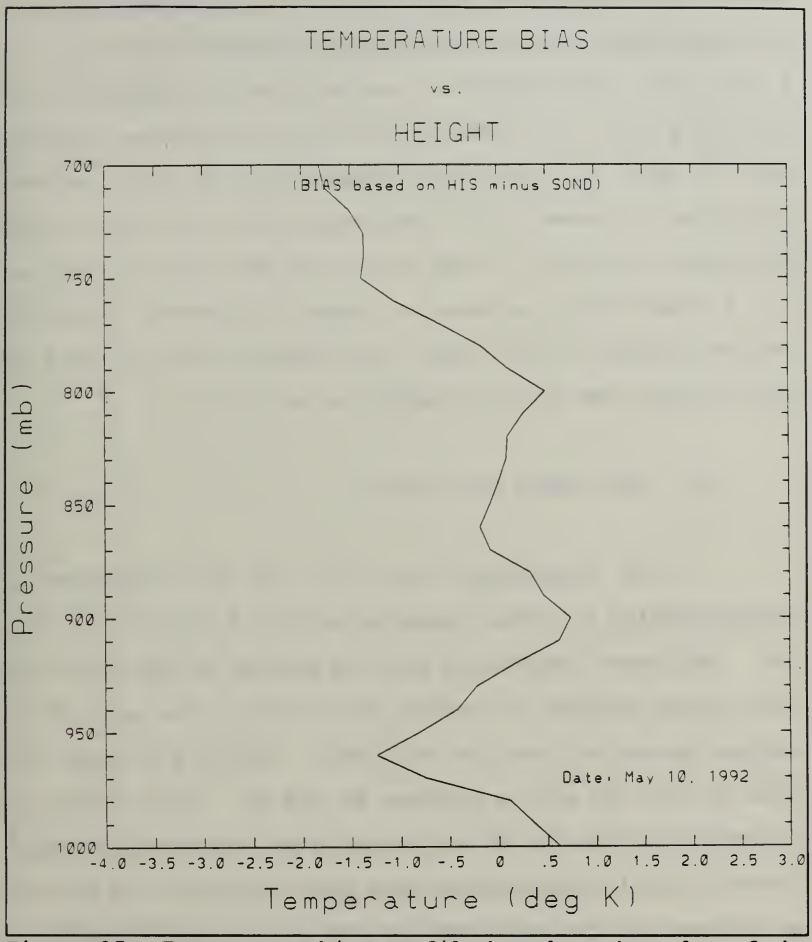

Figure 35: Temperature bias profile based on the value of the HIS minus the value of the rawinsonde at the same level. A positive bias indicates an overestimation and a negative bias an underestimation of the temperature.

earlier. Above the top of the marine inversion the temperature retrievals continues to show a negative bias to the top of the low troposphere with a maximum value of > -3.5 K (Fig. 36). The dewpoint bias is strongly negative on the 10th (Fig. 38) up to the top of the GB-HIS marine inversion due in part to the over compensation of the retrieval algorithm to downwelling IR emittance from intermittent clouds throughout the day. On the 9th in the same layer, there is a 5 - 6 K positive bias when no clouds are present (Fig. 37). On the average for both days, the dewpoint profile had a dry bias through the entire boundary layer (Fig. 39).

b. 1991 Point Sur Cruise

The temperature bias on the 8th indicates an overestimation of actual temperature by 2.5 K at 900 mb (Fig. 40). This warm temperature bias is similar to the 1992 Point Sur cruise because it occurs at the top of a weak GB-HIS marine inversion like the 1992 data. There is a large warm bias on the 8th with a maximum at 820 mb. Even though the atmosphere on the 9th is well-mixed after the frontal passage, there is still a significant warm bias throughout the PBL with a maximum of 3.0 K at 900 mb (Fig. 41). As a result of overestimation of the actual temperature by the GB-HIS on the 8th and the 9th, the overall temperature bias for the 1992 cruise is on average between 1.0 K and 1.5 K (Fig. 42).

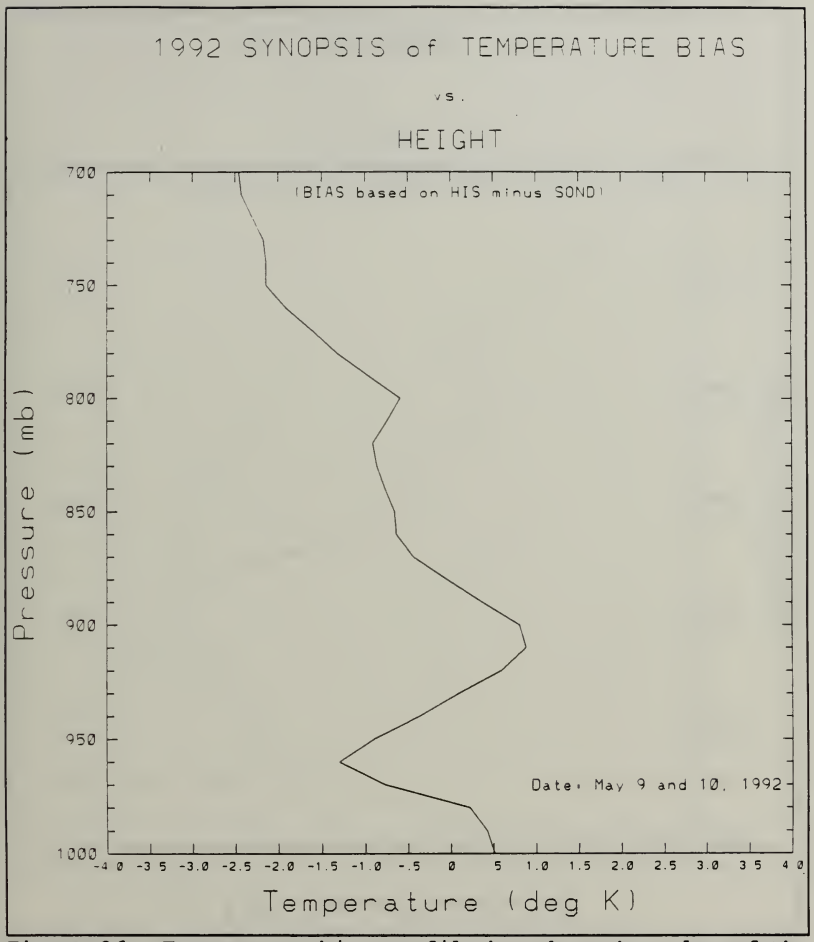

Figure 36: Temperature bias profile based on the value of the HIS minus the value of the rawinsonde at the same level. A positive bias indicates an overestimation and a negative bias an underestimation of temperature.

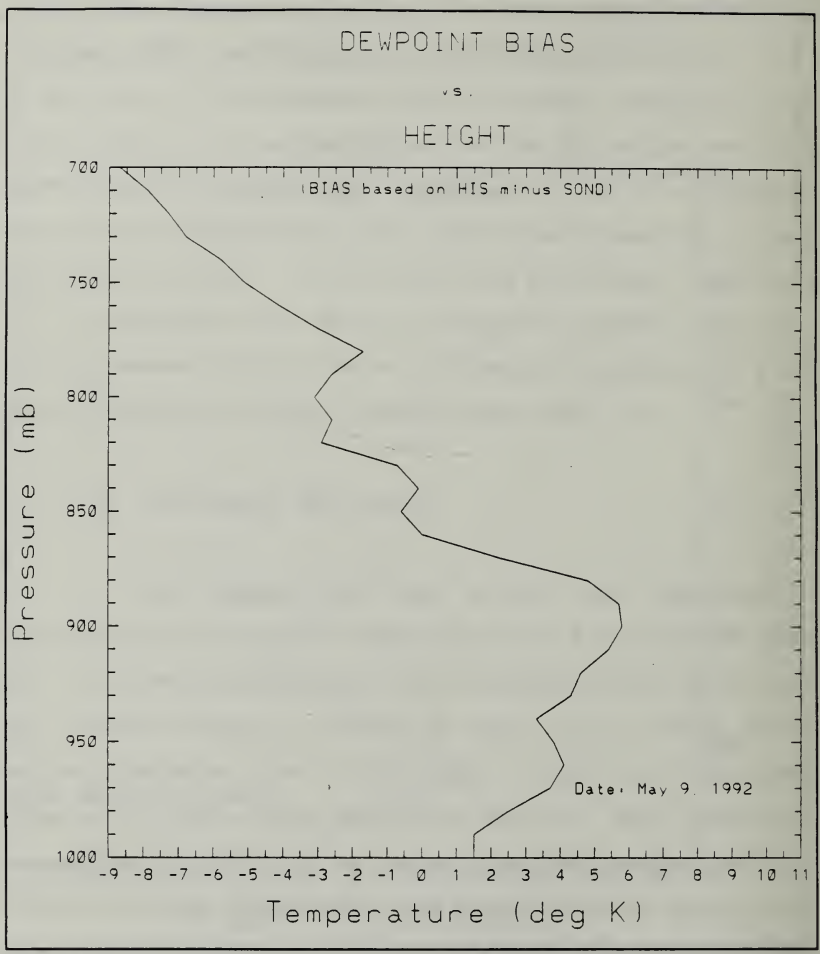

Figure 37: Dewpoint bias profile based on the value of the HIS minus the value of the rawinsonde at the same level. A positive bias indicates an overestimation and a negative bias an underestimation of dewpoint.

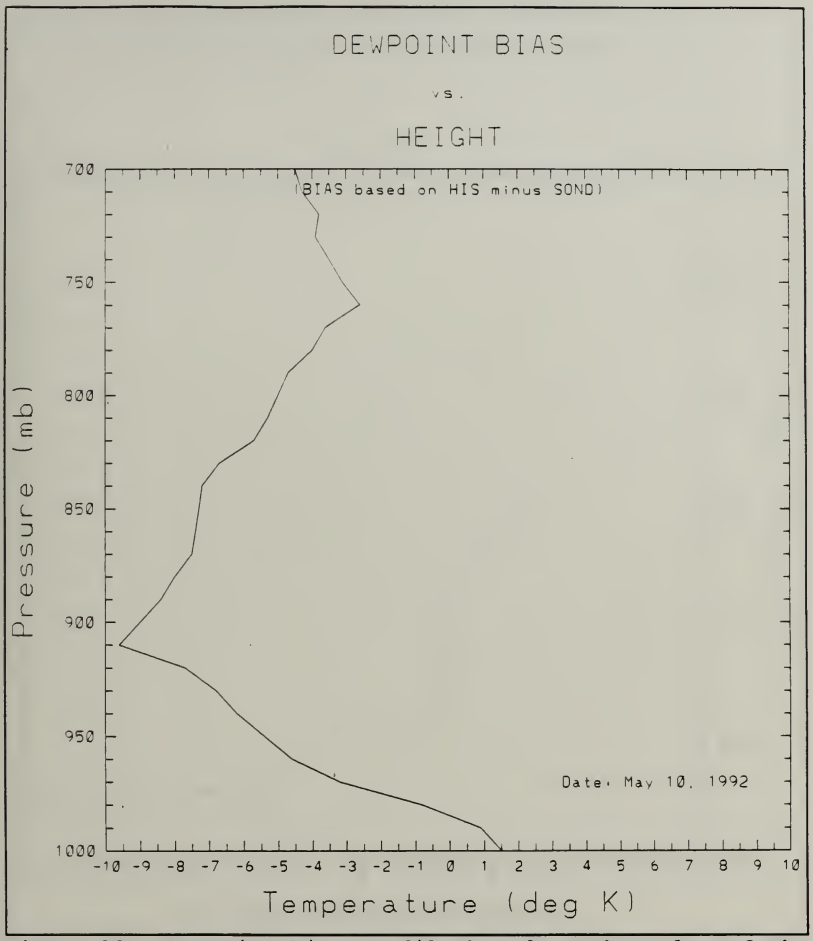

Figure 38: Dewpoint bias profile based on the value of the HIS minus the value of the rawinsonde at the same level. A positive bias indicates an overestimation and a negative bias an underestimation of dewpoint.

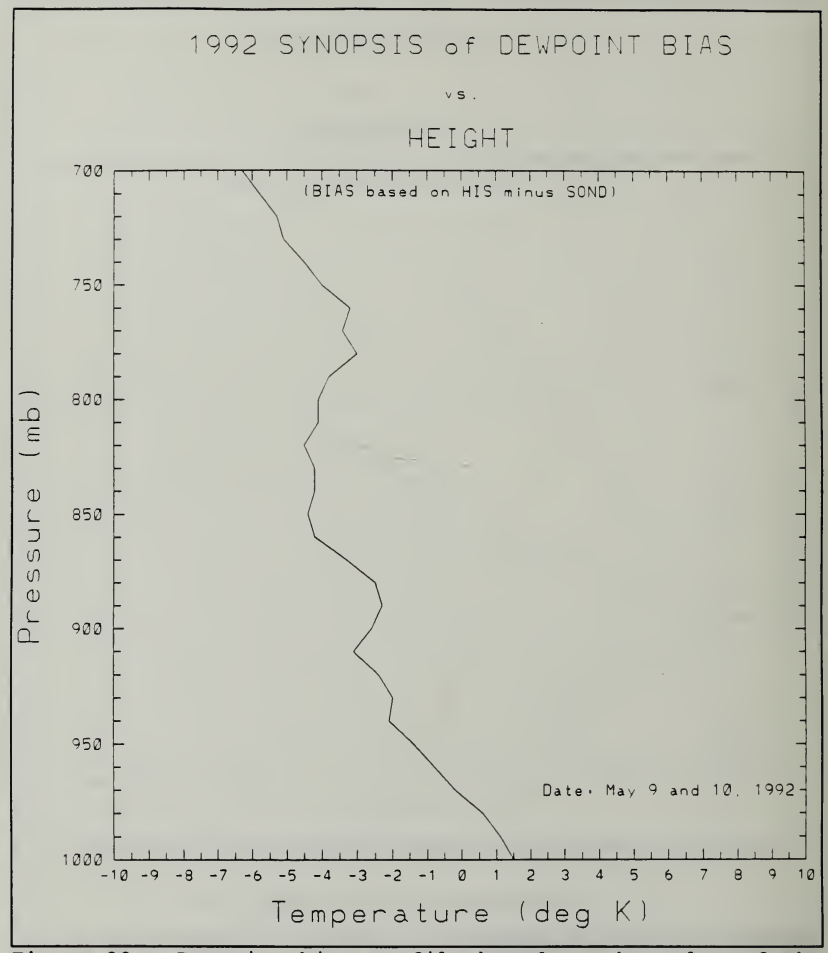

Figure 39: Dewpoint bias profile based on the value of the HIS minus the value of the rawinsonde at the same level. A positive bias indicates an overestimation and a negative bias an underestimation of dewpoint.

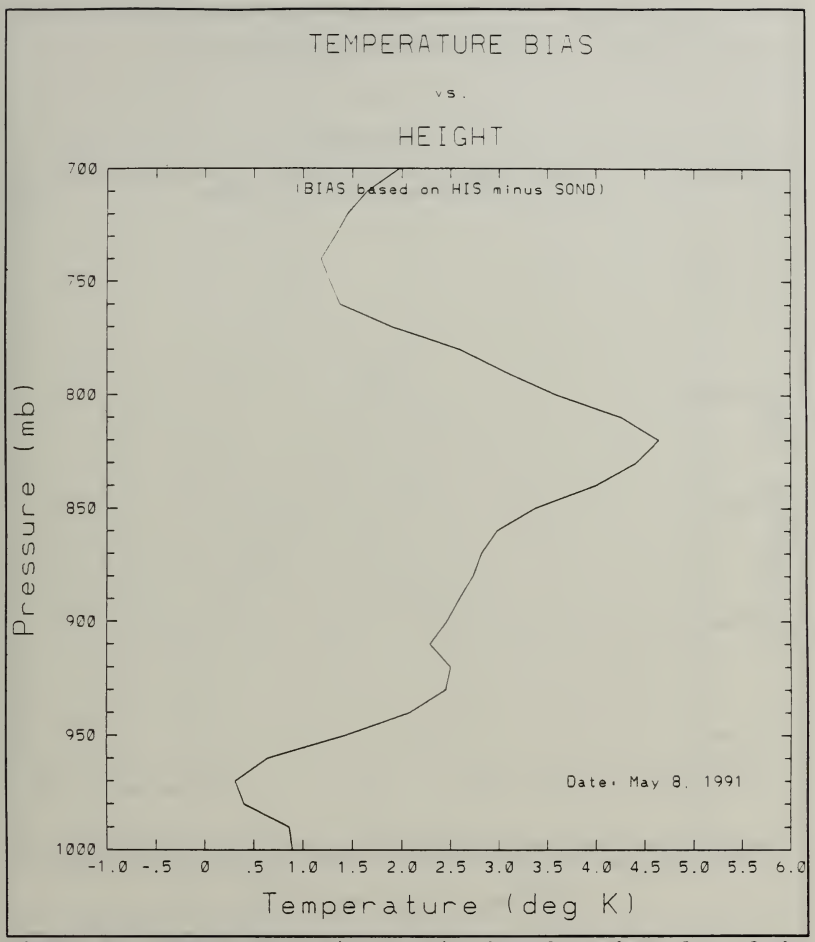

Figure 40: Temperature bias profile based on the value of the HIS minus the value of the rawinsonde at the same level. A positive bias indicates an overestimation and a negative bias an underestimation of temperature.

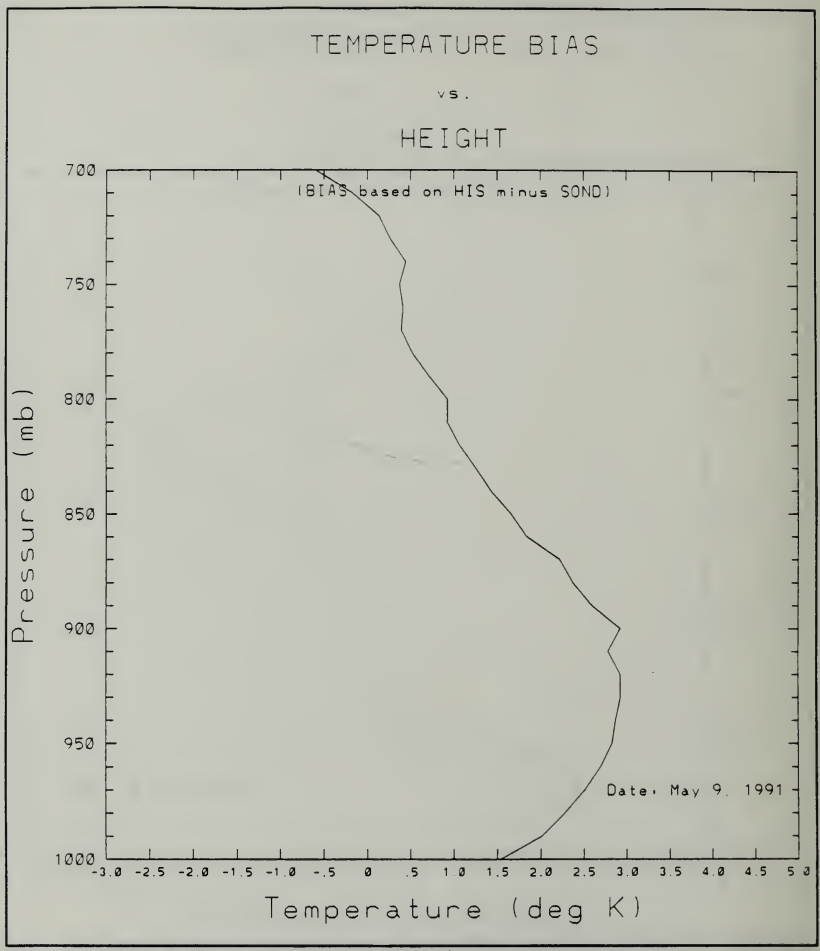

Figure 41: Temperature bias profile based on the value of the HIS minus the value of the rawinsonde at the same level. A positive bias indicates an overestimation and a negative bias an underestimation of temperature.

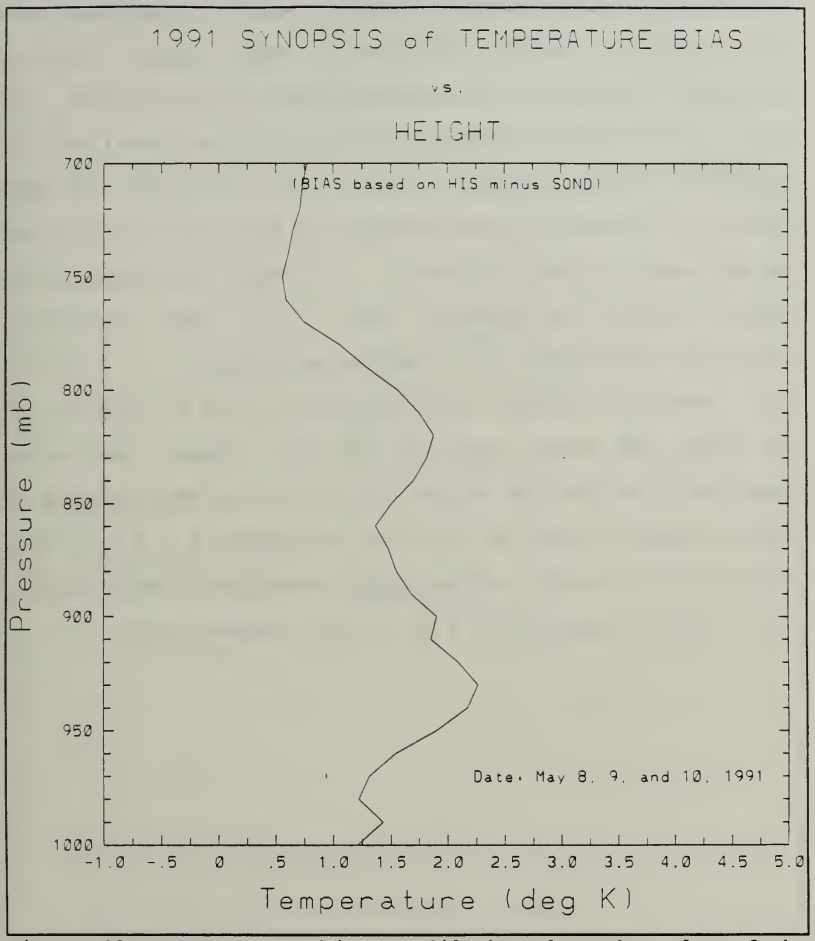

Figure 42: Temperature bias profile based on the value of the HIS minus the value of the rawinsonde at the same level. A positive bias indicates an overestimation and a negative bias an underestimation of temperature.

The dewpoint profiles did not capture the strong subsidence and subsequent drying well. As the front approached on the 8th (Fig. 43), small scale, mid-level moisture fluctuations were underestimated by the GB-HIS. Even as the front was passing, GB-HIS moisture profiles show dewpoint biases of nearly -20 K. In the lower and upper levels a consistent overestimation of moisture is displayed, as was seen in the 1992 data. On 9 May, the dewpoint bias above 820 mb was greater than 5.0 K, and consistently increased with height to a maximum at 700 mb of 17.5 K (Fig. 44). Overall, the mid-level dry bias on the 8th and the mid to upper PBL moist bias on the 9th, shaped the average dewpoint bias for the cruise with the lower PBL showing the least amount of bias up to 900 mb at roughly 1.5 K (Fig. 45). The other two levels, mid and upper, averaged to approximately -7.0 K at 850 mb and 7.0 K at 700 mb, respectively.

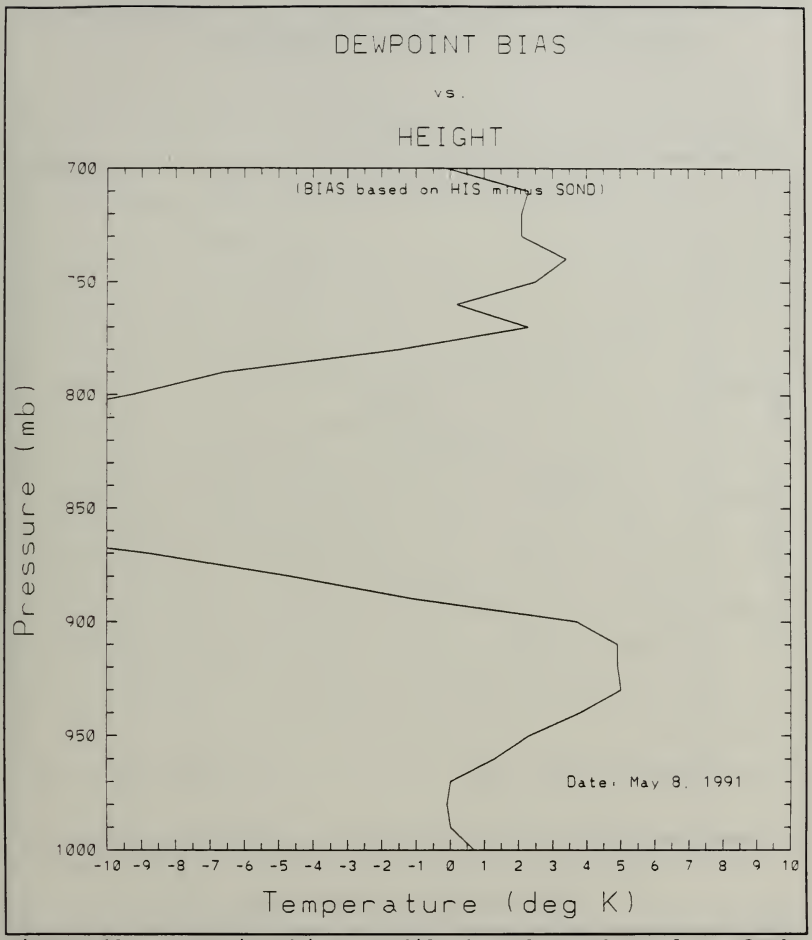

Figure 43: Dewpoint bias profile based on the value of the HIS minus the value of the rawinsonde at the same level. A positive bias indicates an overestimation and a negative bias an underestimation of dewpoint.

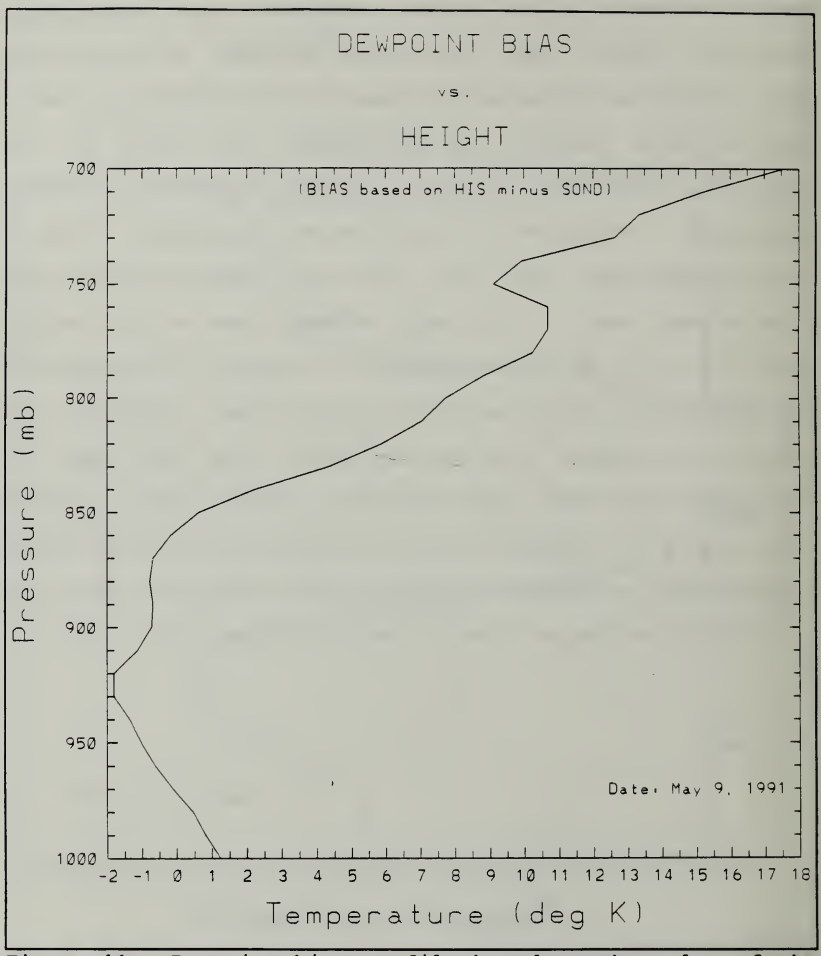

Figure 44: Dewpoint bias profile based on the value of the HIS minus the value of the rawinsonde at the same level. A positive bias indicates an overestimation and a negative bias an underestimation of dewpoint.

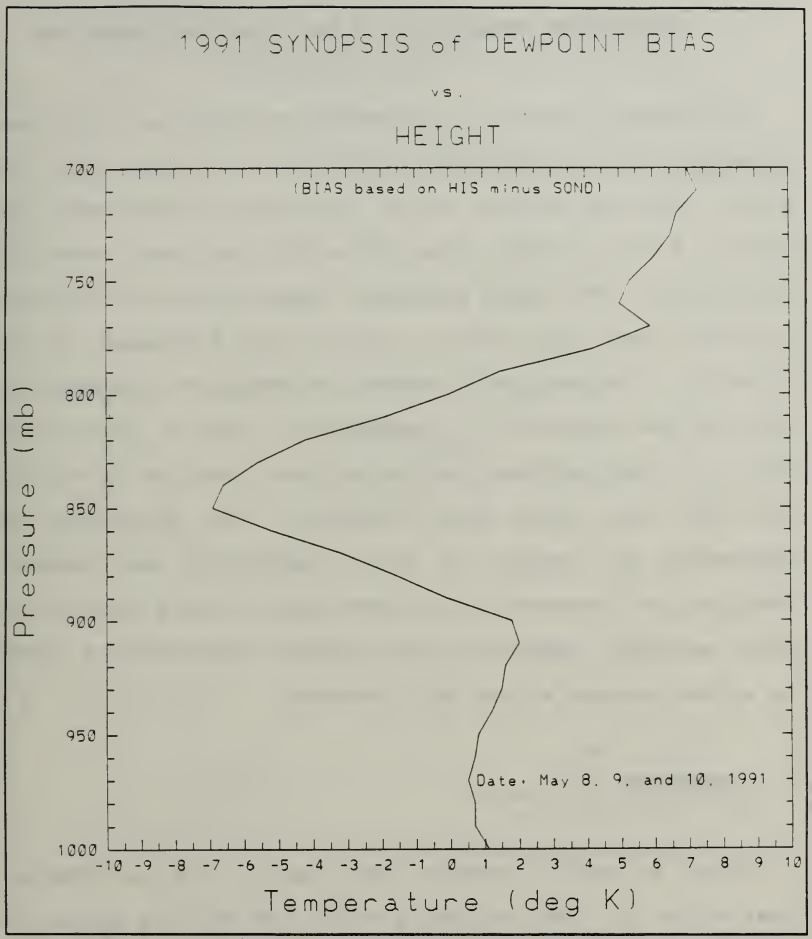

Figure 45: Dewpoint bias profile based on the value of the HIS minus the value of the rawinsonde at the same level. A positive bias indicates an overestimation and a negative bias an underestimation of dewpoint.

V. PRELIMINARY EVALUATION OF NEW RETRIEVAL ALGORITHM

An updated version of the GB-HIS retrieval algorithm was obtained from the University of Wisconsin near the end of the study. The new version has an increase of three more user inputs to the retrieval algorithm which also impact speed and performance. The input parameters used in the new retrieval algorithm and the earlier version are discussed in the appendix. Limited time prevented an extensive investigation of the new version. Consequently, only a statistical evaluation was performed on the retrieval results of both the 1991 and 1992 data sets combined. The strengths and weaknesses are noted for both temperature and dewpoint profiles and compared to the same type of data set for the prior version. Temperature and dewpoint bias profiles showed no strong changes so are not discussed.

A. STRENGTHS

Figs. 46 and 47 present the rms and std dev dewpoint statistics for both cruises for the new and old algorithm. There is obvious improvement in dewpoint retrieval skill (Fig. 46), as skill is achieved throughout almost the entire low troposphere. There is only a shallow layer at the surface of

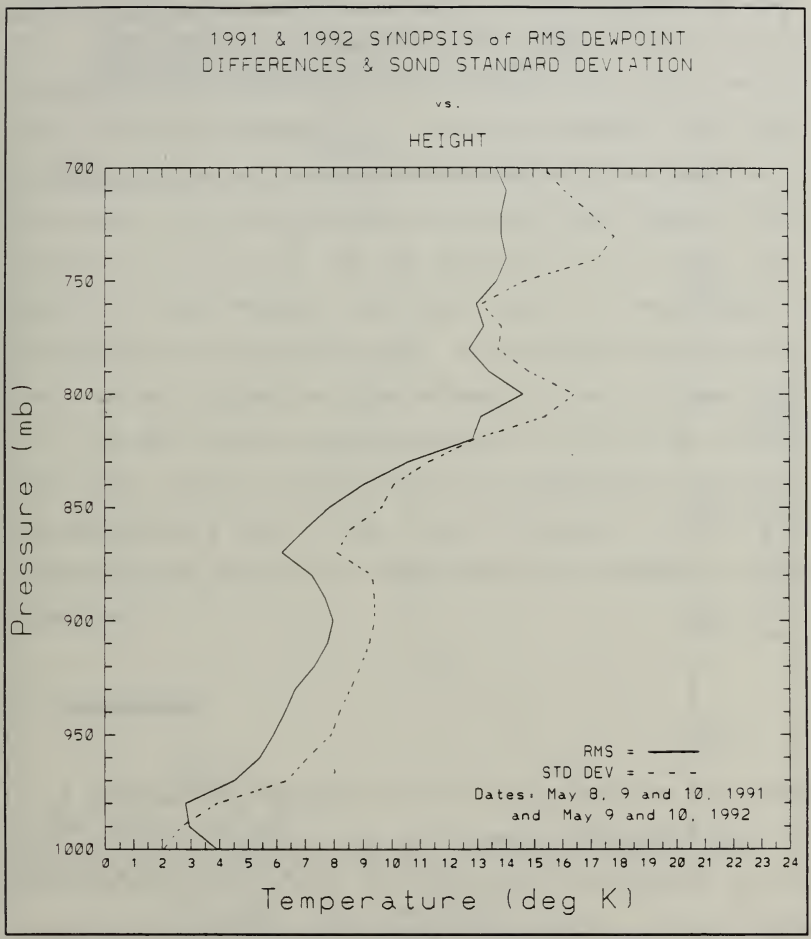

Figure 46: Root mean squared dewpoint differences are compared to atmospheric standard deviation for the 1991 and 1992 cruises combined. Skill is noted when rms is less than std dev. (New Version)

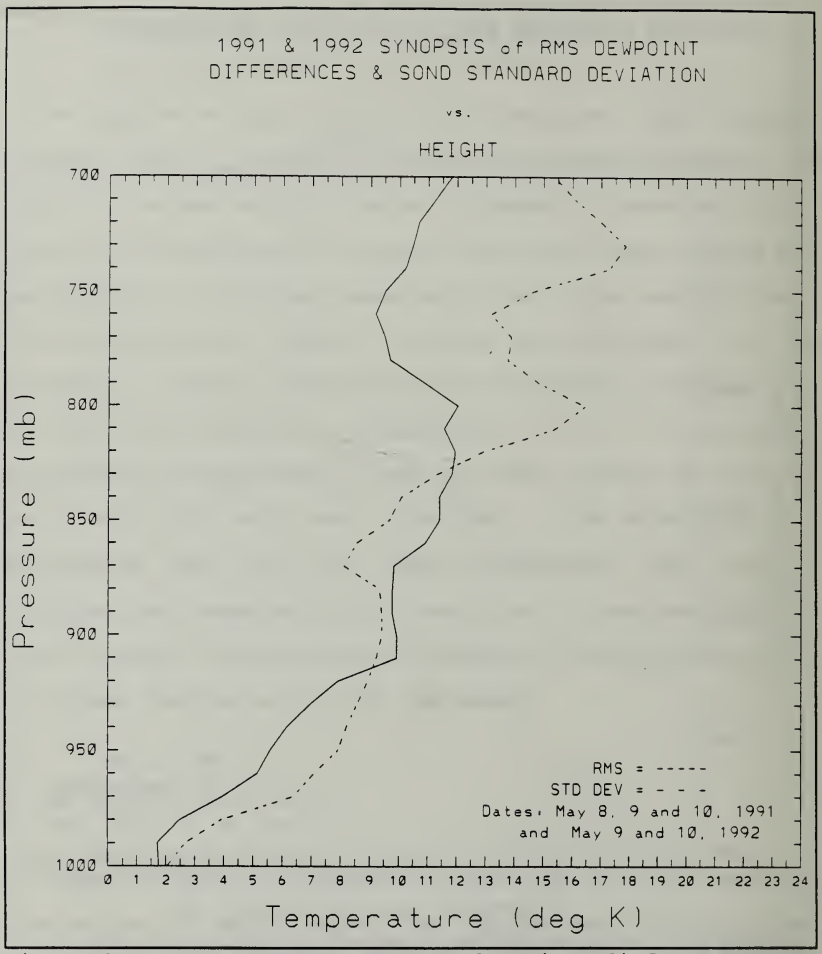

Figure 47: Root mean squared dewpoint differences are compared to atmospheric standard deviation for the 1991 and 1992 cruises combined. Skill is noted when rms is less than std dev. (Old Version)

no skill. This is an improvement on the large no skill layer found in the prior version between 910 mb and 830 mb (Fig. 47). RMS dewpoint differences also improved below 850 mb decreasing from an average of 10.5 K in the prior version (Fig. 47) to an average 7.0 K in the new version (Fig. 46).

Figs. 48 and 49 provide a comparison of the temperature retrievals. RMS temperature differences also improved above 850 mb to 1.5 K (Fig. 48) as opposed to 2.5 K (Fig. 49). These two improvements are also noted in the amount of atmospheric variance explained. In the earlier version there was a no skill moisture layer between 910 mb to 830 mb (Fig. 51), the new version now explains up to 40% of the variance (Fig. 50). Also, the new version of temperature retrievals now maintains a skill level of 60% or greater up to 770 mb increasing the depth of the layer where skill remains greater than 60%.

B. WEAKNESSES

A weakness of the new retrieval algorithm was discovered when visually comparing the new version retrievals with the prior version retrievals, the appropriate rawinsonde profile and the initializing guess rawinsonde profile. In the later part of a 24 h retrieval run, the new version profiles tended to mimic their respective temperature and dewpoint guess profiles which initialized the retrieval algorithm. This

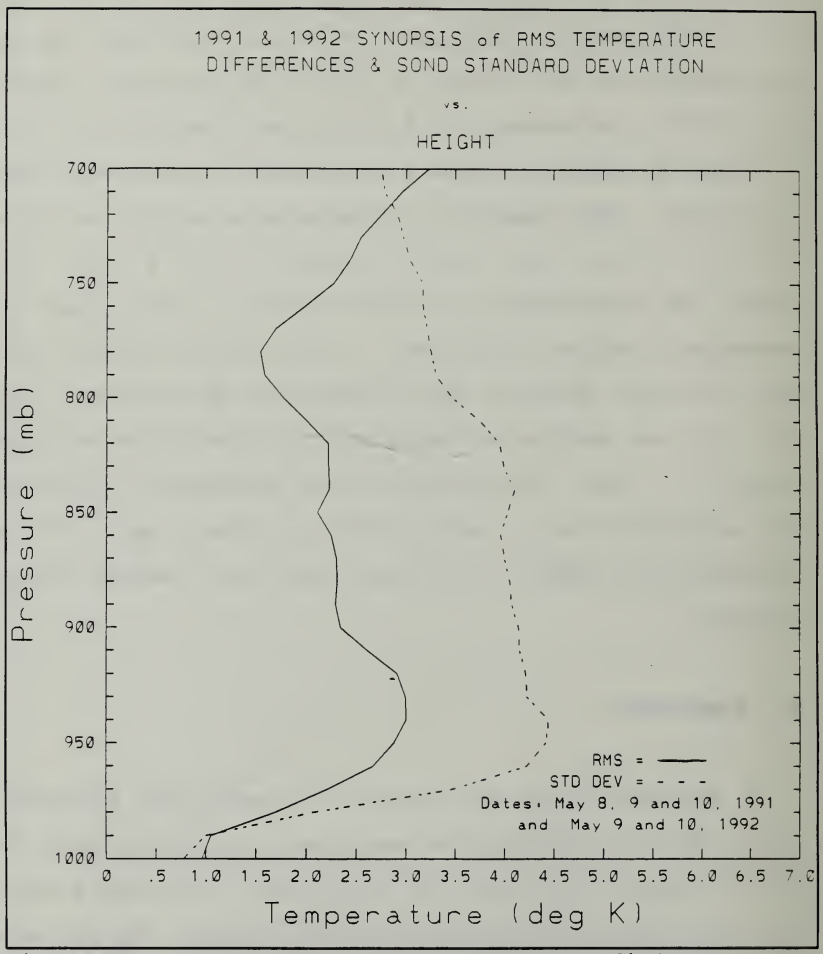

Figure 48: Root mean squared temperature differences are compared to atmospheric standard deviation for the 1991 and 1992 cruises combined. Skill is noted when rms is less than std dev. (New Version)

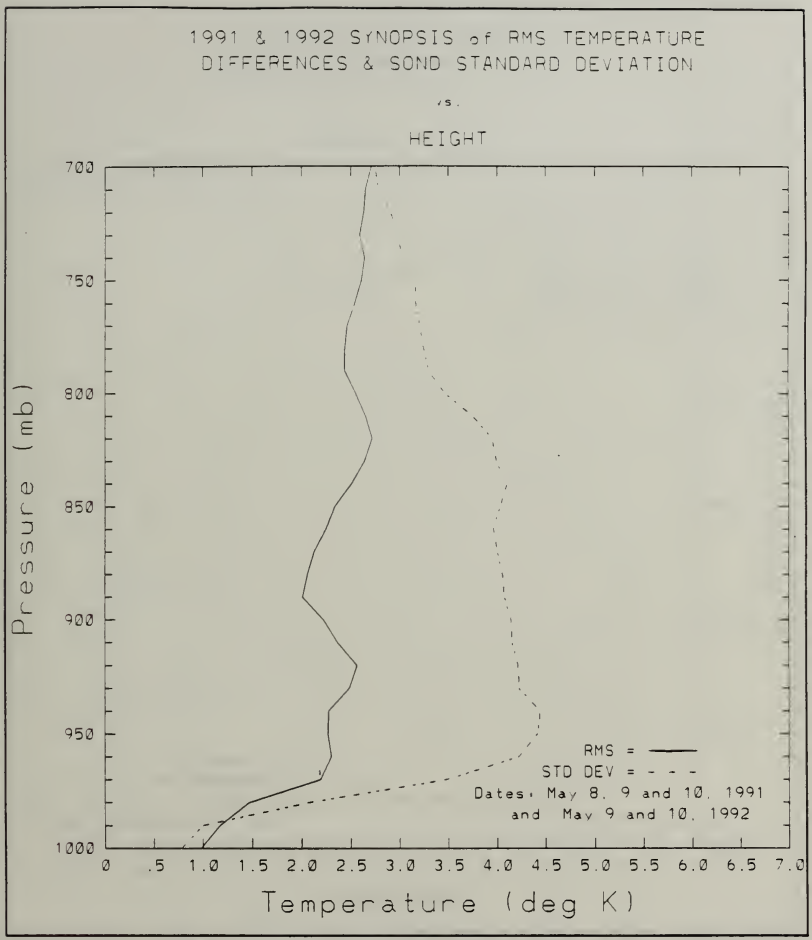

Figure 49: Root mean squared temperature differences are compared to atmospheric standard deviation for the 1991 and 1992 cruises combined. Skill is noted when rms is less than std dev. (Old Version)

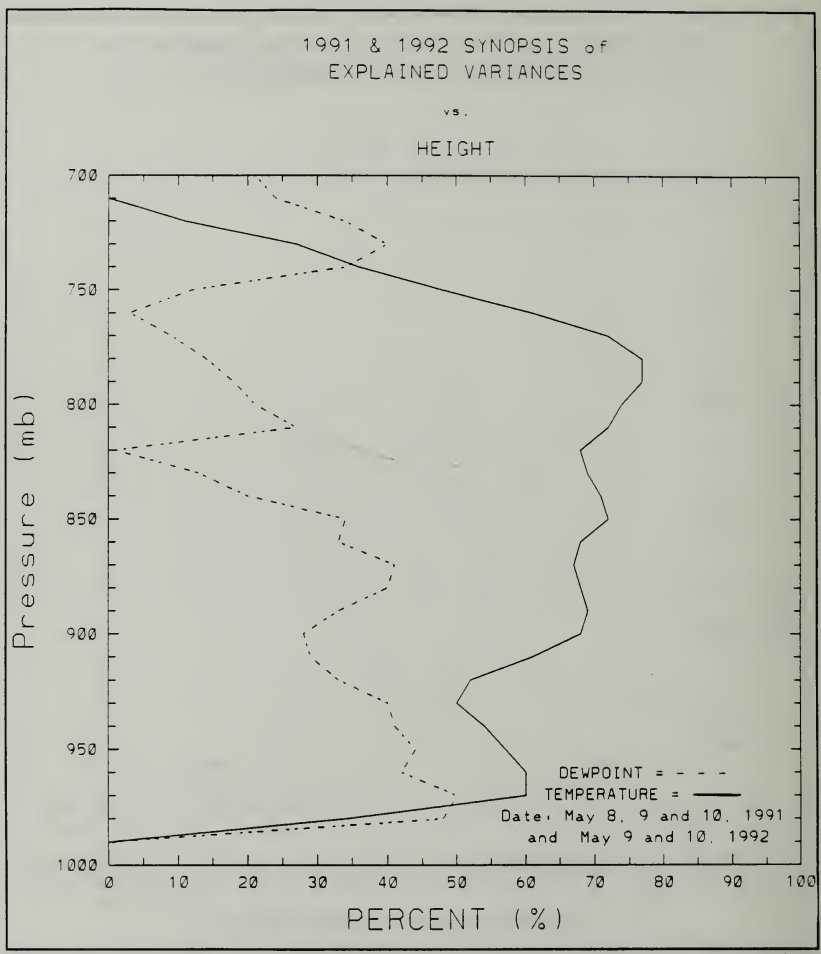

Figure 50: The quantity of atmospheric variance of dewpoint and temperature profiles explained by the HIS. Variance is based on the 0000 GMT rawinsonde profile for each of the days of each cruise. (New Version)

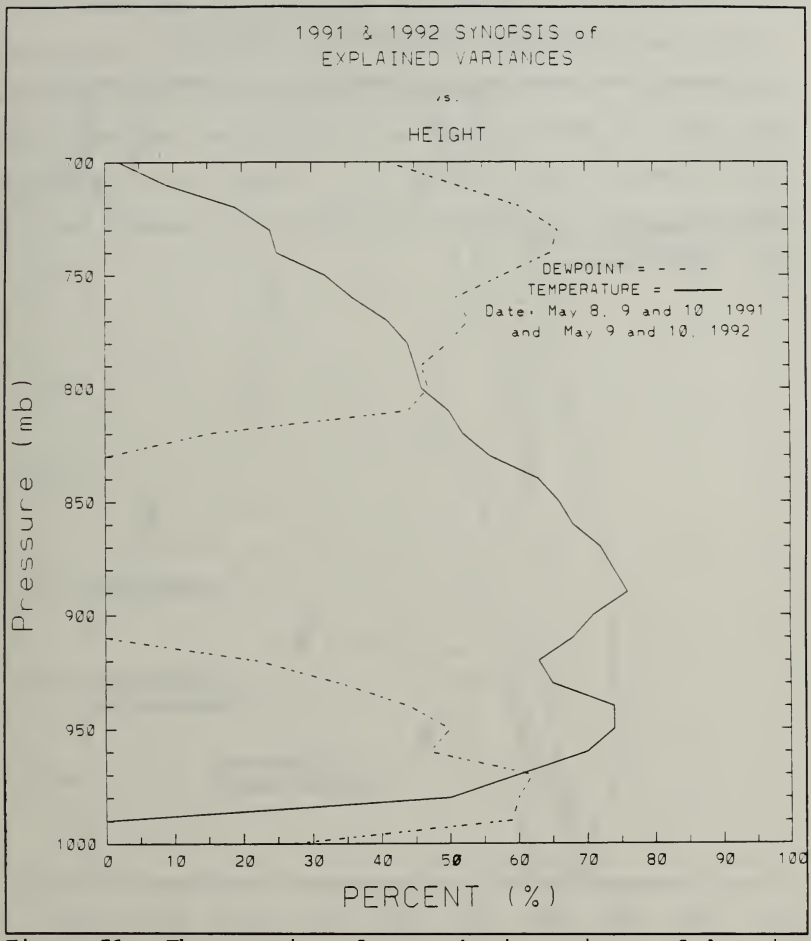

Figure 51: The quantity of atmospheric variance of dewpoint and temperature profiles explained by the HIS. Variance is based on the 0000 GMT rawinsonde profile for each of the days of each cruise. (Old Version)

behavior is illustrated on Fig. 52. Another weakness noted was rms dewpoint differences above 850 mb are about 3.0 K higher over the earlier version (Figs. 46 and 47). Also noted was the skill level achieved on dewpoint profiles below 910 mb and above 830 mb decreased by 10% to 20% as compared to the prior version (Figs. 50 and 51). So some skill is lost in both the upper and lowest layers while improvements occur in the middle levels.

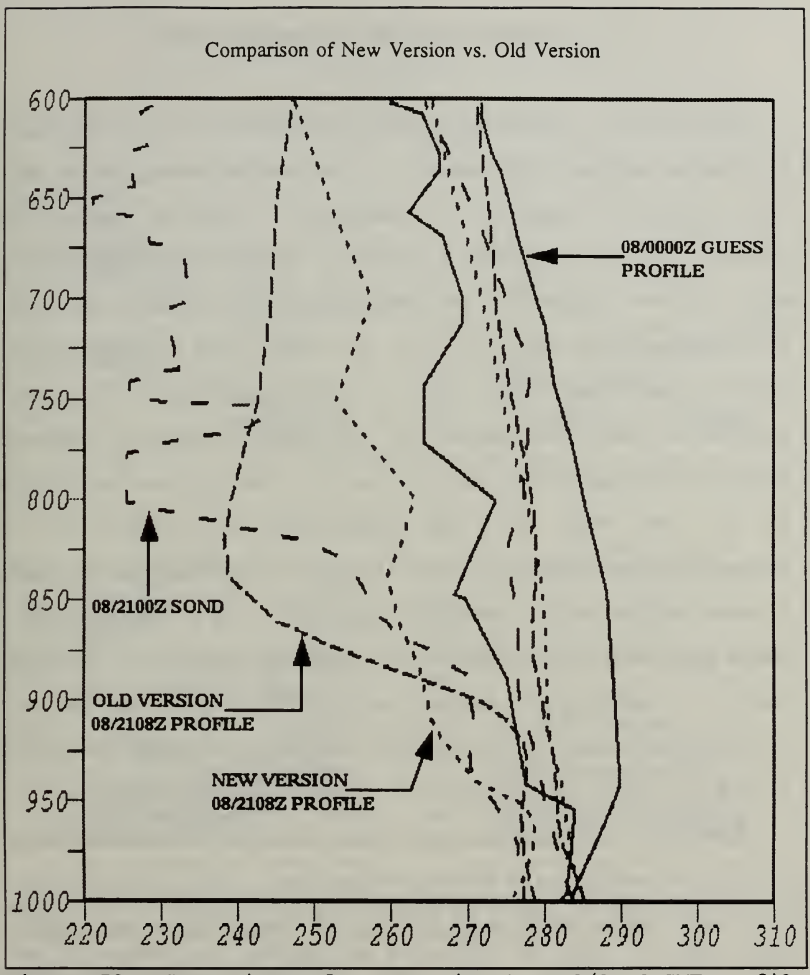

Figure 52: Comparison of new version 910508/2108 GMT profile (small dashed) with old version 910508/2108 GMT profile (medium dashed), 910508/2100 GMT rawinsonde profile (large dashed) and the 910508/0000 GMT guess profile (solid).

VI. CONCLUSION AND RECOMMENDATIONS

This thesis investigated the performance of the GB-HIS in a coastal marine environment. The GB-HIS is found to be a very effective tool for measuring a marine temperature inversion with the overall accuracy (from combining the 1991 and 1992 data sets) of rms temperature differences below 2.5 K throughout the PBL (Fig. 49), and explained variances up to 75% in this layer (Fig. 51). The GB-HIS is a moderately effective tool for measuring the marine surface moisture gradient displaying an overall layer of skill from the surface to 910 mb (Fig. 47) and explaining up to 62% of the atmospheric moisture variance (Fig. 51). Moisture performance is even better with a revised algorithm. As a consequence of these two conclusions, from a military perspective, the GB-HIS can be a militarily significant tool for refractive duct forecasting (Fig. 53) by noting air mass changes associated with the rising or lowering of refractive ducts aloft.

However, improvements are required in moisture retrievals to capture small scale moisture features. Plus, overall skill is modest explaining only of 75% of temperature and 66% for dewpoint profiles. The new retrieval algorithm shows improvements in both moisture and temperature. With additional investigation and research resulting further improvements, the GB-HIS has the potential to be a wealth of

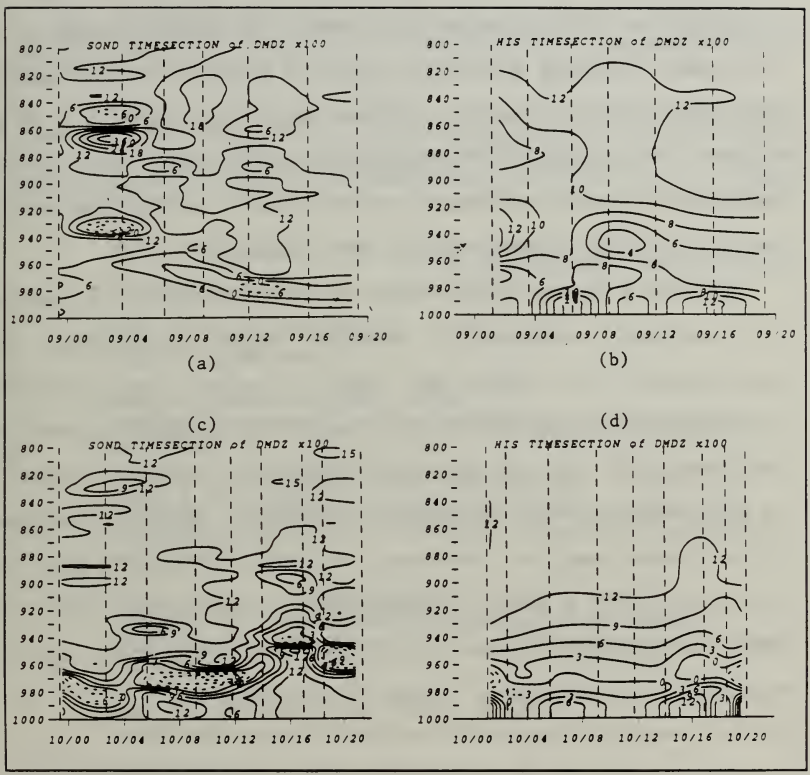

Figure 53: Timesections of $\delta M/\delta Z$ on 9 and 10 May 1992 for the rawinsonde, (a) and (c), and the GB-HIS, (b) and (d), data. $\delta M/\delta Z$ values are scaled by a factor of 100. Dashed lines indicate negatives values.

tactical atmospheric information for all Department of Defense resources.

Recommendations for further investigation are: 1) to investigate the effects of multiple iterations on retrieval accuracy, 2) to determine the affect of marine aerosols on retrieval accuracy and how they also affect the systematic environmental bias used in the retrieval algorithm, and 3) to discover the impact the systematic environment bias has on retrieval accuracy and whether this bias is fairly constant or variable in the coastal marine environment.

These are viewed to be three of the more major influences to retrieval accuracy. Because these influences are interrelated, it would be best to study one influence initially then progress to the others. To better evaluate the performance of the new retrieval algorithm, more data needs to be acquired to lessen the impact of specific weather phenomena on retrieval results. For long term study of the GB-HIS, the acquisition of a GB-HIS instrument is recommended for the Naval Postgraduate School to receive continuous data and for deployment on additional research cruises.

APPENDIX

RETRIEVAL ALGORITHM USER INPUT PARAMETERS

This appendix describes the possible input parameters for the new and prior retrieval algorithms and the choices made for these parameters for both version's retrieval run.

The following are the prompts for the nine user input parameters for the previous retrieval algorithm along with the actual choices made (parameters marked with "*" are not considered part of the nine user inputs which affect the speed or performance, they provide only input/output information):

*a. ENTER path for output (\ must end string !):
C:\GBRET\RESULT\HIS91\MAY10\
(location of output retrievals)

b. WANT TO OMIT RETRIEVAL? [Y,N]: N
(self-explanatory)

c. WANT TO SMOOTH GUESS? [Y,N]: Y
(smooth out small scale features in rawinsonde profile)

d. ENTER # OF PASSES,PLO,PHI,MID-WEIGHT: 1 1000. 600. 5.
(number of passes, pressure of lowest level for retrieval, pressure of highest level for retrieval, unsure of use)

e. ENTER TOTAL # ITERATIONS ("0" for 1 RET.): 0
(number of iterations to produce a retrieval - inactive in older version, but implemented in newer version)

f. WANT TO INCLUDE BIAS (OBS - CALC) ? Y
(systematic environmental bias used increase accuracy)

g. WANT TO SHIFT GUESS PROFILE ? N
(shift guess profile ahead in time to use as a guess for each retrieval instead of the previous retrieval)

h. Use Surface Observations ? Y (for 1992 data)
or N (for 1991 data)
(use surface temperature from self-calibration - not available on instrument used on 1991 cruise)

*i. OBSERVED (APODIZED,RADIANCE) SPECTRUM:
C:\GB-HIS\DATA\HIS91\PTSUR91.RA3
(location of interferogram or observed radiance file)

j. DO YOU WANT TO EXCLUDE ANY REGIONS? [Y,N]: Y
ENTER LIMITS OF SPECTRAL REGION [W1,W2]: 482 525
DO YOU WANT TO EXCLUDE ANY REGIONS? [Y,N]: Y
ENTER LIMITS OF SPECTRAL REGION [W1,W2]: 665 675
DO YOU WANT TO EXCLUDE ANY REGIONS? [Y,N]: Y
ENTER LIMITS OF SPECTRAL REGION [W1,W2]: 745 1408
DO YOU WANT TO EXCLUDE ANY REGIONS? [Y,N]: N
(exclude regions of IR spectrum from calculations)

k. ENTER RET. TOP P., GAMMA, CRIT0: 700. .0005 5.
(top pressure level of retrieval, a matrix smoothing parameter to force the retrieval and the guess profile to merge at the top pressure level, unsure)

*l. ENTER Input Record Number Range: 183 205
(the record numbers of the radiances observed throughout a day)

*m. ENTER File Name of Output MS File: 910510F1.MSF
(name of output file used with other University of Wisconsin software)

The choices made here remained constant for all retrieval runs using the older version except where noted in paragraph h and in the parameters used for input/output.

The following are the prompts for the 12 user input parameters for the previous retrieval algorithm along with the actual choices made (parameters marked with "*" are not considered part of the 12 user inputs which affect the speed or performance, they provide only input/output information):

*a. Same as above.

b. Same as above.

c. Same as above.

d. Same as above, but different values used:
1 1000. 100. 1.

e. Same as above. This is now implemented, but not used.

f. Same as above.

g. Same as above.

h. Same as above.

*i. Same as above.

j. DO YOU WANT MORE TEMPERATURE REGIONS? [Y,N]: Y
ENTER LIMITS OF SPECTRAL REGION [W1,W2]: 606 660
DO YOU WANT MORE TEMPERATURE REGIONS? [Y,N]: Y
ENTER LIMITS OF SPECTRAL REGION [W1,W2]: 675 735
DO YOU WANT TEMPERATURE REGIONS? [Y,N]: N
(include regions of IR spectrum for calculations)

DO YOU WANT MORE WATER REGIONS? [Y,N]: Y
ENTER LIMITS OF SPECTRAL REGION [W1,W2]: 560 660
DO YOU WANT MORE WATER REGIONS? [Y,N]: Y
ENTER LIMITS OF SPECTRAL REGION [W1,W2]: 675 760
DO YOU WANT MORE WATER REGIONS? [Y,N]: N
(include regions of IR spectrum for calculations)

k. Same as above, but different values used:
600. .001 10.

*l. Same as above.

*m. Same as above.

o. ENTER AEROSOL ht (KM) AND VISIBILITY (KM): 0 0
(thickness of aerosol layer and surface visibility - values used here essentially deactivate the impact of aerosols and visibility)

p. ENTER BIAS WEIGHT (0 - 1): 0.5
(weight the effect the systematic environmental bias has)

q. ENTER T and TD-CONSTRAINT (K): 1000 1000
(constraints to the amount retrieval temperature and dewpoint values can differ from the previous retrieval which is its guess profile; exceeding this limit causes the current retrieval to be averaged with the 0000 GMT rawinsonde guess profile - values used here will prevent exceeding the constraints)

The choices made here remained constant for all retrieval runs using the newer version except where noted in paragraphs d, e, h, and k, the additional new parameters and in the parameters used for input/output.

LIST OF REFERENCES

Martinez, A.A., 1991: High frequency analyses of coastal meteorological phenomena affecting refractivity. Naval Postgraduate School, Monterey, California, pp. 1-87.

Revercomb, H.E., H. Bujis, H.B. Howell, D.D. LaPorte, W.L. Smith, and L.A. Sromovsky, 1988: Radiometric calibration of IR Fourier transform spectrometers: solution to a problem with the high-resolution interferometer sounder. *Appl. Opt.*, **27**, pp. 3210-3218.

Smith, W.L., H.E. Revercomb, H.B. Howell, H.M. Woolf, R.O. Knuteson, R.G. Decker, M.J. Lynch, E.R. WestWater, R.G. Strauch, K.P. Morgan, B. Stankov, M.J, Falls, J. Jordan, M. Jacobsen, W.F. Dabberdt, R. McBeth, G. Albright, C. Paneitz, G. Wright, P.T. May, and M.T. Decker, 1990: GAPEX: A ground-based atmospheric profiling experiment. *Bull. Amer. Meteor. Soc.*, **71**, pp. 310-318.

Smith, W.L., H.E. Revercomb, H.B. Howell, H.-L. Huang, R.O. Knuteson, E.W. Koenig, D.D. LaPorte, S. Silverman, L.A. Sromovsky, and H.M. Woolf, 1990: GHIS - The GOES high-resolution interferometer sounder. *J. Appl. Meteor.*, **29**, pp. 1189-1204.

Smith, W.L., H.E. Revercomb,R.O. Knuteson, H.B. Howell, and F.A. Best, 1992: Remote sensing of the planetary boundary layer with a high-resolution interferometer sounder. Submitted to *J. Appl. Meteor.*

INITIAL DISTRIBUTION LIST

		No. Copies
1.	Defense Technical Information Center Cameron Station Alexandria, VA 22304-6145	2
2.	Library, Code 52 Naval Postgraduate School Monterey, CA 93943-5000	2
3.	Chairman (Code MR/Hy) Department of Meteorology Naval Postgraduate School Monterey, CA 93943-5000	1
4.	Professor Carlyle H. Wash (Code MR/WX) Department of Meteorology Naval Postgraduate School Monterey, CA 93943-5000	4
5.	Captain Steven A. Rugg PSC 1, Box 99999 Offutt Air Force Base, NE 68113	1
6.	Program Manager Air Force Institute of Technology Wright-Patterson Air Force Base, OH 45433	1
7.	Commander Air Weather Service Scott Air Force Base, IL 62225	1
8.	Commanding Officer Air Force Global Weather Central Offutt Air Force Base, NE 68113	1
9.	Air Weather Service Technical library Scott Air Force Base, IL 62225-5008	1
10.	Dr. Juergen Richter, Code 54 NRAD 71 Catalina Blvd. San Diego, CA 92152	1